universität wien

MASTERARBEIT / MASTER'S THESIS

Titel der Masterarbeit / Title of the Master's Thesis

„Characterization of potential cancer initiating cells in breast cancer cell lines“

verfasst von / submitted by

Timo Hagen, BSc

angestrebter akademischer Grad / in partial fulfilment of the requirements for the degree of

Master of Science (MSc)

Wien, 2015 / Vienna 2015

Studienkennzahl lt. Studienblatt / degree programme code as it appears on the student record sheet:	A 066 863
Studienrichtung lt. Studienblatt / degree programme as it appears on the student record sheet:	Masterstudium Biologische Chemie UG2002
Betreut von / Supervisor:	Univ.-Prof. Dipl.-Ing. Dr. Manfred Ogris
Mitbetreut von / Co-Supervisor:	Julia Maier, MSc

Thanks to all members of the MMCT laboratory who supported me over the last half year. Especially I want to thank my advisor Julia Maier for her guidance in all matters. I also want to thank Prof. Ogris for facilitating me to join his lab and for his kind support.

Table of Contents

1. Introduction

1.1 Cancer stem cells (CSCs) as key components in malignant disease

Cancer is the second most common cause of death in Europe after circulatory disease (Eurostat Database, 2015). Breast cancer alone caused a high death rate of 33.3 per 100 000 female EU-28 inhabitants in 2012 and was the type of cancer with the highest incidence as well as the second highest mortality rate after lung cancer (Eurostat). Considering these facts, metastasizing breast cancer is a very important field of research.

Recurrent and metastatic breast cancer present the most common breast cancer-related deaths (O'Shaughnessy, 2005). Only 6% of newly diagnosed cases present metastatic breast cancer, however, approximately 30% of early stage diagnosed women with breast cancer develop metastatic or recurrent advanced disease (National Institute of Health, seer.cancer.gov, 2015). To understand metastasizing breast cancer we have to take a look at the cellular-level. First a few important terms in cancer biology have to be explained: transformed cells/cancer cells and cancer stem cells or tumor-initiating cells. Transformed cells arise through several alterations (Ruddon, 2003). Cells undergo cytologic changes including increased number and size of nuclei, increased nucleus:cytoplasmic ratio, and formation of clusters and cords of cells (Ruddon, 2003). Transformed cells become immortal, meaning that they can passaged indefinitely (Ruddon, 2003). Also, they lose their anchorage dependence and acquire the ability to grow in non-adherent environment like soft agar (Ruddon, 2003). This malignant transformation facilitates the formation of a cancer cell.

Cancer stem cells (CSCs) are a novel subclass of neoplastic cells within tumors (Hanahan and Weinberg, 2011). Studies over the last years have proposed that the characteristics of CSCs are immortality, tumor-initiation, self-renewing and pluripotency (Reya et al., 2001). These characteristics are supposed to lead to tumor development, metastasis and recurrence (Chen et al., 2013). CSCs have been identified in various solid tumors, such as

breast cancer, colon cancer or lung cancer (Chen et al., 2013). The presence of CSCs in primary lesions from breast cancer patients after the application of neoadjuvant chemotherapy has shown to predict poor survival (Sakakibara et al., 2012). Considering the mentioned facts about CSCs, the research on them is essential and they could display an attractive target for clinical cancer treatments.

Several intrinsic mechanisms of chemoresistance confer CSCs an integral role in recurrence following chemotherapy (Abdullah and Chow, 2013). ABC transporter expression, such as P-glycopotein (MDR1) and breast cancer resistance protein (ABCG2) is one mechanism providing chemoresistance in CSCs (Chow et al., 2012; Scharenberg et al., 2002; Shapiro et al., 1997). Doxorubicin and related drugs are effluxed by both of these ABC transporters (Abdullah and Chow, 2013). Some other drugs like paclitaxel are only effluxed by MDR1 and not ABCG2 (Chow et al., 2012; Litman et al., 2000). Another ability of CSCs providing chemoresistance is aldehyde dehydrogenase (ALDH) activity (Abdullah and Chow, 2013). ALDH expression confers resistance to the cytostatic cyclophosphamide in CSCs (Sreerama and Sladek, 1997). Several signaling pathways like Wnt/β-catenin, Hedgehog or Notch also contribute to CSC biology including chemoresistance (Abdullah and Chow, 2013). For instance, the Wnt/β-catenin signaling pathway enables chemoresistance to 5-fluoruracil and doxorubicin in CSCs (Flahaut et al., 2009; Noda et al., 2009). Due to the numerous intrinsic mechanisms of resistance in CSCs it is likely necessary to target more than one of these pathways operating in CSCs (Naujokat and Steinhart, 2012). Such a treatment approach could eradicate all CSCs and decrease the probability of escape mutants (Liu and Wicha, 2010; Mueller et al., 2009; Park et al., 2009; Zhou et al., 2009).

In order to study CSCs in detail, the isolation of this cell subpopulation is necessary (Chen et al., 2013). Surface biomarker phenotypes can be used to differentiate between CSCs, other tumor cells or normal stem cells (Chen et al., 2013). The isolation of CSCs by fluorescence-activated cell sorting (FACS) based on cell surface markers or intracellular molecules is applied most frequently at the moment (Chen et al., 2013). The $CD44^{+}/CD24^{low/-}$ subpopulation of breast cancer cells in solid tumors was proposed to comprise a population containing breast cancer stem cells (BCSCs) (Al-Hajj et al., 2003). This was indicated by a greater capacity for tumor formation in NOD/SCID mice (Al-Hajj et al., 2003). Since the finding of Al-Hajj and colleagues, sorting of breast cancer cells by their CD24/CD44 surface phenotype

has been used to isolate or enrich for tumorigenic BCSCs (Grimshaw et al., 2008). More recently the overexpression of a promising CSC marker, adhesion molecule α-6 integrin (CD49f), was detected in a stem cell-like subpopulation of breast cancer cell lines (Cariati et al., 2008). Owing to the findings in the literature, the relatively novel CD49f BCSC surface marker was selected in addition to the established marker combination CD24/CD44 for this master's thesis. To analyze the described surface marker profile, it was aimed at establishing a time-efficient and reproducible flow-cytometry-based method.

The antigenic phenotype has been shown to correlate with the cell morphology. A relationship between CD24 antigenic phenotype and cell morphology, meaning a luminal-like appearance for $CD24^+$ cell lines and a basal/mesenchymal appearance for $CD24^-$ cell lines, has been documented (Fillmore and Kuperwasser, 2008). As such, breast cancer cell lines exhibiting different cell morphologies were analyzed with respect to their CD24 antigenic profile in this master's thesis.

Another important characteristic of BCSCs is the transition between alternative states, distinct epithelial-like (mesenchymal-epithelial transition, MET) and mesenchymal-like (epithelial-mesenchymal transition, EMT) states (Liu et al., 2014). Depending on the state BCSCs can perform various functions, epithelial-like BCSCs are centrally located proliferative cells, whereas mesenchymal-like BCSCs are mainly quiescent cells which are located at the tumor invasive front (Liu et al., 2014). The transition between EMT- and MET-like states confers the BCSCs with properties important for disease progression, like tissue invasion, dissemination, and growth at metastatic sites (Liu et al., 2014).

Based on molecular profiling breast cancers are subdivided into categories with distinct biological and clinical characteristics (Riaz et al., 2009). Luminal breast cancers, which express the steroid hormone receptors progesterone receptor (PR) and estrogen receptor (ER), HER2 positive breast cancers and basal breast cancers that are triple negative (TN) (Riaz et al., 2009). TN means that they do not express hormone receptors or show amplification of the HER2 gene (Riaz et al., 2009). Depending on this classification the therapy approach, such as hormone therapy, HER2 blockade, or chemotherapy is chosen (Liu et al., 2014). From a clinical point of view the triple negative or HER-2 positive breast cancers have a poorer prognosis than hormone receptor expressing breast cancers (Brenton et al., 2005). Liu and co-workers found

that similar gene-expression profiles in BCSCs across molecular subtypes of breast cancer are present, which suggests that BCSCs targeting drugs could be used across molecular subtypes of cancer (Liu et al., 2014).

1.2 Salinomycin as CSC inhibitor

The seminal study of Gupta and co-workers showing that the antibiotic salinomycin preferentially targets the viability of CSCs within $CD44^{high}/CD24^{low}$ antigenic phenotype subpopulation in breast cancer cells in mice aroused worldwide interest to perform further research on this drug (Gupta et al., 2009). Additionally CSC-associated genes correlating with poor-prognosis tumors have been shown to be lost upon salinomycin treatment (Gupta et al., 2009). Further studies have documented that salinomycin effectively kill CSCs in different types of human cancers in vitro and in xenograft mice bearing human cancers (Basu et al., 2011; Zhang et al., 2011, 2012). Treatment of $CD44^{+}/CD24^{-}/ALDH1^{+}$ human BCSCs with salinomycin, as well as the combination of salinomycin with the chemotherapeutic doxorubicin, markedly increased apoptosis (Gong et al., 2010). In addition the eradication of human breast cancer in xenograft mice was significantly enhanced by combination of salinomycin with the conventional anticancer drug paclitaxel while reducing the number of $CD44^{+}/CD24^{-}$ BCSCs in tumors (Zhang et al., 2012). Due to this promising studies salinomycin was therapeutically applied in a pilot clinical trial with a small group of metastatic cancers (Steinhart et al., 2012). The outcome was a partial regression of tumor metastasis and minor side effects together with conventional chemotherapeutics (Steinhart et al., 2012). As a consequence Verastem Inc. was envisioned to start a phase I/II clinical trial using the proprietary formulation of salinomycin termed VS-507 in patients with triple negative breast cancer in 2013 (Naujokat and Steinhart, 2012). However, the outcome of this clinical trial is not yet clear. Taken together, strong evidence has been accumulated that salinomycin alone and particularly in combination with conventional cytostatic drugs effectively targets CSCs (Naujokat and Steinhart, 2012).

In this master's thesis the doxorubicin related drug daunorubicin of the anthracycline family was used in addition to the CSC-targeting drug salinomycin. Similar to doxorubicin,

daunorubicin is capable of DNA intercalation and stops the DNA replication as well as the DNA transcription by inhibiting topoisomerase II (Pang et al., 2013). Based on the literature, it was expected that the application of the combination of daunorubicin with salinomycin reveals higher cytotoxicity than the drugs alone.

In the last years several studies were aiming at the discovery of the mechanisms of salinomycin's effect against human CSCs (Naujokat and Steinhart, 2012). These studies have contributed to a basic understanding of some mechanisms, however to uncover the exact mechanisms further studies are needed (Naujokat and Steinhart, 2012). It has been shown that salinomycin can induce apoptosis in human BCSCs (Gong et al., 2010), is a potent inhibitor of ABC transporters in different cancer cells (Kim et al., 2012; Riccioni et al., 2010), and is unlikely to become a substrate of ABC transporters because it is rapidly embedded in biological membranes (Mitani et al., 1976). Furthermore salinomycin has been documented to downregulate the Hedgehog-Gli1 self-renewal pathway in $CD44^+/CD24^-$ human BCSCs (Lu et al., 2015). Salinomycin promotes the K^+ efflux from mitochondria and cytoplasm because it acts as K^+ ionophore (Mitani et al., 1976, 1975; Pressman and Lattanzio, 1978). Considering that pharmacological induction of K^+ efflux leads to apoptosis and cytotoxicity in cancer cells (Andersson et al., 2006; Bortner et al., 1997), it can be assumed that mitochondrial and cytoplasmic K^+ efflux induced by salinomycin (Li et al., 2008; Park et al., 2010) results in the apoptosis of CSCs (Naujokat and Steinhart, 2012). Considering the mentioned characteristics of salinomycin, we decided to test the effect of this CSC-targeting drug on cancer cell lines exhibiting different degrees of CSC properties in this master's thesis.

1.3 Non-adherent colony formation assays

To understand the principle behind non-adherent colony formation assays, anoikis has to be explained. When apoptosis is induced by the lack of a correct cell/ECM (extracellular matrix) attachment it is termed anoikis (Gilmore, 2005). Due to anoikis normal cells are not able to grow anchorage-independent, whereas transformed cells can grow and divide irrespective of their surrounding environment (Borowicz et al., 2014). The capability to grow in non-adherent environment can be evaluated with different non-adherent colony formation

assays using semi-solid material such as soft agar, methyl cellulose or matrigel. In this semi-solid environment visible colonies called spheroids or multicellular aggregates can only form when originating from a transformed cell (Borowicz et al., 2014). Non-adherent mammospheres of transformed cells, formed when cells possess the ability to proliferate in suspension, are even mainly composed of the cancer stem cell subpopulation (Hirsch et al., 2009). The high capability of CSCs to grow in non-adherent environment (Hirsch et al., 2009) represents a key principle for this master's thesis. Non-adherent colony formation assays facilitate the assignment of CSC properties depending on the growth capability of the tested cells.

The selection of material depends on the type of application. Matrigel is a basement membrane-like extracellular matrix extract which contains various growth factors, including fibroblast growth factor, transforming growth factor beta and epidermal growth factor (Benton et al., 2011). Especially during metastasis most epithelial originating tumors interact with the basement membrane matrix (Benton et al., 2011). That is why colony formation assays using matrigel are usually aiming at a more physiological environment than other assays using other materials, such as soft agar or methyl cellulose. Due to the batch variations of matrigel, it is very difficult to maintain exactly the same environment among the experiments leading to problems with reproducibility. The purpose of our assay was to examine basic CSC properties, leading us to assume that a reductionist approach without surplus growth factors would be best suited.

The soft agar colony formation assay is a well-established method to monitor anchorage-independent growth and is quick and easy to perform (Borowicz et al., 2014). In the soft agar colony formation assay spheroids form from single cells, mimicking tumor development. The methyl cellulose assay represents a faster method for obtaining multicellular aggregates than with the soft agar colony formation assay (Bilandzic and Stenvers, 2014). However, spheroids form from more than one cell disabling the monitoring of tumor development. The methyl cellulose assay has the ability to provide multicellular aggregates in a more rapid fashion than its single-cell-based counterparts, ideally suited for testing out multistep processing methods such as histological cryosections that allow antigen determination. For the mentioned reasons it was decided to use soft agar as well as methyl cellulose for the non-adherent colony formation assay in this work.

2. Aim of the thesis

In this master's thesis our intention was to establish a method for the antigenic phenotype determination of breast cancer cell lines. We were aiming at a convenient, time-efficient, antibody-amount-saving and reproducible flow cytometry-based method which can be carried out in a 96-well plate format.

CSC surface marker were used, as we focused on the verification of CSC properties. Owing to the findings in the literature, the relatively novel CD49f BCSC surface marker was selected in addition to the established marker combination CD24/CD44.

We chose the two basal type triple negative MDA-MB-231 and MDA-MB-436, as well as the luminal type ER-HER2-PR positive breast cancer cell line MCF7 for our experiments. All three tested breast cancer cell lines resemble breast cancers with poor prognosis, and there is an urgent need to perform research on them.

We also wanted to test the effect of chemotherapeutic treatments to the breast cancer cell lines. In addition to the CSC-targeting drug salinomycin, doxorubicin related drug daunorubicin of the anthracycline family was used for the treatment. Based on the literature, we expected that the application of the combination of daunorubicin with salinomycin reveals higher cytotoxicity than the drugs alone.

Non-adherent colony formation assays were introduced to test the growth ability of breast cancer cells in non-adherent environment. The high capability of CSCs to grow in non-adherent environment (Hirsch et al., 2009) represents a key principle for this master's thesis. The purpose of our assay was to examine basic CSC properties, leading us to assume that a reductionist approach without surplus growth factors would be best suited. Therefore we decided to use soft agar as well as methyl cellulose for the non-adherent colony formation assay instead of matrigel. Furthermore we intended to test the growth ability of salinomycin pre-treated breast cancer cells in non-adherent environment.

3. Material and Methods

3.1 Media

DMEM high glucose 10% FBS:

Dulbecco's Modified Eagle's Medium – low glucose (Sigma-Aldrich®, D5546, St. Louis, MO, USA)

10% Fetal Bovine Serum (Sigma-Aldrich®, F7524, St. Louis, MO, USA)

Addition of 3.5 g/l D(+)-Glucose (Merck Millipore®, 346351, Darmstadt, GER)

0.584 g/l L-Glutamin by addition of 200 mM L-Glutamin solution (Sigma-Aldrich®, G7513, St. Louis, MO, USA)

3.2 Reagents

Table 1. List of reagents.

Name	Product number, supplier, location
Agarose, low gelling temperature	A9414, Sigma-Aldrich®, St. Louis, MO, USA
Bovine Serum Albumin (BSA)	A9647, Sigma-Aldrich®, St. Louis, MO, USA
Crystal Violet	C3886, Sigma-Aldrich®, St. Louis, MO, USA
Daunorubicin	D8809, Sigma-Aldrich®, St. Louis, MO, USA
Dimethyl sulfoxide (DMSO)	D8418, Sigma-Aldrich®, St. Louis, MO, USA

Dulbecco's Modified Eagle's Medium – low glucose	D5546, Sigma-Aldrich®, St. Louis, MO, USA
Dulbecco's Modified Eagle's Medium - low glucose (powder)	D5523, Sigma-Aldrich®, St. Louis, MO, USA
Dulbecco's Phosphate Buffered Saline	D8537, Sigma-Aldrich®, St. Louis, MO, USA
Ethylenediaminetetraacetic acid (EDTA)	E6758, Sigma-Aldrich®, St. Louis, MO, USA
Electran® Agarose DNA Pure Grade	443666A, VWR®, Radnor, PA, USA
Fetal Bovine Serum (FBS)	F7524, Lot No. 064M3396, Sigma-Aldrich®, St. Louis, MO, USA
D(+)-Glucose	Merck Millipore®, 346351, Darmstadt, GER
L-Glutamine solution 200 mM	G7513, Sigma-Aldrich®, St. Louis, MO, USA
Hoechst 34580	63493, Sigma-Aldrich®, St. Louis, MO, USA
Methyl cellulose	M0512, Sigma-Aldrich®, St. Louis, MO, USA
Paraformaldehyde	A3813.1000, VWR®, Radnor, PA, USA
4-(2-hydroxyethyl)-1-piperazineethanesulfonic acid (HEPES)	A3724.0500, VWR®, Radnor, PA, USA
Salinomycin	S4526, Sigma-Aldrich®, St. Louis, MO, USA
Sodium bicarbonate	S5761, Sigma-Aldrich®, St. Louis, MO, USA
Sodium chloride	A2942.500, VWR®, Radnor, PA, USA
Thiazolyl Blue Tetrazolium Bromide (MTT)	M2128, Sigma-Aldrich®, St. Louis, MO, USA
TrypLE™ Express (1X)	12605010, Gibco®, Grand Island, NY, USA
Versene™ 1:5000 (1X)	15040033, Gibco®, Grand Island, NY, USA

3.3 Cell maintenance

For our experiments we used three two human breast cancer cell lines from the American Type Culture Collection (ATCC®, Manassas, VA, USA) and one human breast cancer cell line from the European Collection of Cell Cultures (ECACC®, Salisbury, UK) . All three cell lines stem from the mammary gland/breast and were derived from the metastatic site of adenocarcinomas via pleural effusion. MDA-MB-231 cell line (ATCC®, Lot/Batch No. 62235654, Original passage from manufacturer: 38; PO No. 710405391) is classified as mesenchymal, MDA-MB-436 cell line (ATCC®, Lot/Batch No. 61331460, Original passage from manufacturer: 19, PO No. 710405391) as myoepithelial and MCF7 cell line (ECACC®, Original passage from manufacturer: 18, Product No. 86012803 Sigma-Aldrich®) as luminal cell type. Cell lines with passage numbers of 44-58 for MDA-MB-231, 26-36 for MDA-MB-436 and 14-21 for MCF7 were used in our experiments.

All three cell lines were cultured in 25/75/150 cm^3 cell culture flasks (USA Scientific, CC7682-4825/75/15, Ocala, FL, USA) with DMEM high glucose 10% FBS in humidified incubator at 37 °C and 5% CO_2. Upon confluency, the spent medium was discarded and the cells were washed with PBS (Sigma-Aldrich®, D8537, St. Louis, MO, USA). The MCF7 cell line was incubated with TrypLE™ Express (Gibco®, 12605010, Grand Island, NY, USA) for 5 minutes in humidified incubator at 37°C and 5% CO_2. The MDA-MB-231 and MDA-MB-436 cell line was incubated with Versene™ (Gibco®, 15040033, Grand Island, NY, USA) for 3 minutes in humidified incubator at 37°C and 5% CO_2. The three cell lines were detached by gently tapping, collected with DMEM high glucose 10% FBS and transferred into a centrifuge tube for centrifugation for 5 minutes at 200 xG. The obtained pellet was resuspended in DMEM high glucose 10% FBS and the desired fraction was added to the new cell culture flask containing DMEM high glucose 10% FBS.

3.4 Antibodies

Table 2. Primary antibodies used for CSC characterization.

Target, label	Product number, manufacturer
CD24, PE	555428, BD Biosciences®
CD44, Alexa Fluor 647	103018, BioLegend®
CD49f, Brilliant Violet 421	562582, BD Biosciences®
CD24-isotype, PE	555574, BD Biosciences®
CD44-isotype, Alexa Fluor 647	400626, BioLegend®
CD49f-isotype, Brilliant Violet 421	562602, BD Biosciences®

3.5 CSC marker evaluation

The cells were detached with Versene™ according to chapter 3.3, resuspended in 5 ml DMEM high glucose 10% FBS and 10 µl of the cell suspension were diluted 1:10 with PBS to determine the cell number using haemocytometer (Marienfeld-Superior®, 0640010, Lauda-Königshofen, GER). The cells were spun down at 200 xG for 5 minutes, the medium was aspirated and the remaining pellet was resuspended in the amount of PBS needed to obtain 2.86 x 10^6 cells/ml. To seed 200 000 cells per well of a 96 V-bottom plate, 70 µl of cell suspension were deposited in each well. The cells were spun down at 600 xG for 5 minutes and the PBS was aspirated. The reagent PEB was prepared with PBS, 2mM EDTA (Sigma-Aldrich®, E6758, St. Louis, MO, USA) and 0.5% BSA (A9647, Sigma-Aldrich®, St. Louis, MO, USA). The antibody master mix (isotype or target antibodies (AB)) was freshly compounded on ice in the dark. Each antibody staining was performed as singlet. The composition for one treatment was as follows: 4.0 µl CD24 (PE), 1.0 µl (1:10 in PEB) CD44 (Alexa Fluor 647), 1.0 µl CD49f (Brilliant Violet 421) and 14.0 µl PEB. 20 µl of appropriate antibody master mix were added per well. After thoroughly suspending the plate was incubated for 30 minutes at 4 °C with a lid. The cells were spun down at 600 xG 4 °C for 5 minutes, the liquid was aspirated and the pellet was washed once with ice-cold PBS. The cells were spun down at 600 xG 4 °C for 5 minutes, the PBS was aspirated and the pellet was resuspended well in 100 µl ice-cold PEB.

The measurement was performed using MACSQuant® Analyzer 10 with the following settings: FSC: 236 V; SSC: 306 V; B2 (CD24): 360 V; V1 (CD49f): 308 V; R1 (CD44): 360 V; sample volume 100 µl; uptake volume 90 µl. The obtained data was analyzed with FlowJo™ V.10.0.8. In all plots debris was gated out before subsequent analysis. Through the gating strategy only single cells were considered (Figure 2).

3.6 Chemotherapeutic treatments

The cells (MCF7, MDA-MB-231) were treated with 0.2% (v/v) DMSO (Sigma-Aldrich®, D8418, St. Louis, MO, USA), daunorubicin (Sigma-Aldrich®, D8809, St. Louis, MO, USA) or salinomycin (Sigma-Aldrich®, S4526, St. Louis, MO, USA) at doses of 0.5, 1.0 and 2.0 µM. The treatments were prepared from the following stock solutions: 1.0 mM salinomycin in DMSO (stored at 4 °C) and 12 mM daunorubicin in ddH_2O (stored at 4 °C). The combination of salinomycin and daunorubicin was also tested at 2.0 µM. Each condition was tested as singlet. After 4 days of treatment the cells were passaged in an adjusted ratio and allowed to recover for 4 days in the absence of compound (Gupta et al., 2009). Thus it was ensured that any further toxicity in the continued presence of compound would not confound the results (Dong et al., 2011). The medium was renewed every day during the recovery phase. After the determination of the cell number with a haemocytometer, CSC marker evaluation (Chapter 3.5) and soft agar colony formation assay (Chapter 3.7) was carried out with all conditions where enough viable cells were left.

3.7 Non-adherent colony formation assay

For the soft agar colony formation assay a modified protocol of Borowicz et al. was used (Borowicz et al., 2014). The assay was carried out in non-adherent 6-well plates (USA Scientific, CC7672-7506, Ocala, FL, USA). The untreated cells were seeded in duplicates, pre-treated cells in singlets. The bottom layer was set to 0.5% normal agarose (VWR®, 443666A, Radnor, PA, USA) and the top layer to 0.3% low melting point agarose (Sigma-Aldrich®, A9414,

St. Louis, MO, USA). After pouring the bottom layer the agarose was allowed to gel at 4 °C for 45 minutes. For all three cell lines (MDA-MB-231, MDA-MB-436, MCF7) 5000 cells per well were seeded. After the standard growth time of 21 days (Borowicz et al., 2014) in humidified incubator (37 °C, 5% CO_2), the spheroids were fixed with 4% (w/v) formaldehyde in HBS for 60 minutes at 37 °C. To prepare the 4% (w/v) formaldehyde fixation solution, paraformaldehyde (VWR®, A3813.1000, Radnor, PA, USA) was dissolved at 60 °C under magnetic stirring in HBS (20 mM HEPES, 150 mM NaCl, pH 7.1). After adjusting pH to 7.0-7.5, the mixture was filtered through a pleated filter and stored at 4 °C. After that the spheroids were stained with 0.005% crystal violet in PBS for 30 minutes at room temperature. To count the spheroids photos were taken with a camera. In order to determine the size of the spheroids, 4x magnified images using Motic AE31 series microscope with Moticam 3.0MP (Motic Electric, Xiamen, China) were taken of spheroid samples and evaluated in ImageJ®.

For the methyl cellulose assay a protocol of Bilandzic and Stenvers was used (Bilandzic and Stenvers, 2014). The methyl cellulose stock solution was prepared according to the protocol (Bilandzic and Stenvers, 2014) and diluted 1:5 with DMEM high glucose 10% FBS. To this mixture the appropriate amount of MDA-MB-231 single cell suspension was added. 150 µl of cell containing methyl cellulose-media-mixture were pipetted into each well of a 96 well U-bottom microplate (greiner bio-one™, 650101, Frickenhausen, GER). Cell number of 1000, 2500 and 4167 was tested in the pilot assay. Each cell number was tested in octets. After 24 hours of growing in humidified incubator (37 °C, 5% CO_2) images were taken using Motic AE31 series microscope with Moticam 3.0MP (Motic Electric, Xiamen, China) at 4x magnification. The size of the multicellular aggregates was determined in ImageJ®.

3.8 Cell viability stain

In a 96-well plate (greiner bio-one™, 655180, Frickenhausen, GER) 7500 cells per well were seeded and cultured overnight in humidified incubator 37 °C 5% CO_2. On the next day the spent medium was discarded and the cells treated with different conditions. For each cell line the following treatments were tested: Solvent control 0.2% (v/v) DMSO (duplicates), 2.0/1.0/0.5 µM salinomycin (triplicates). The cells were cultured for 72 h in humidified

incubator (37 °C, 5% CO_2) and photos taken at 4x or 10x magnification. The live-dead determination was carried out using a PI staining solution and MACSQuant® Analyzer 10 in a 96-well V-bottom plate format. The total concentration of PI was 0.005 mg/ml. PI staining solution was added directly prior to the measurement on ice. The obtained data was analyzed with FlowJo™ V.10.0.8. In all plots debris was gated out before subsequent analysis. Through the gating strategy only single cells were considered (Figure 2). The threshold for PI positive cells was set to > 17 on logarithmic scale of B3 PerCP-Vio700-A channel. The statistical evaluation was performed with Microsoft Excel®. The bars represent the arithmetic mean of the measurements and the error bars the standard deviation (SD).

4. Results

4.1 Optimization of the CSC marker staining

First, an antibody titration using the breast cancer cell line MDA-MB-231 was performed. The goal was to find the right amount of antibodies needed for each marker. Therefore 25%, 50% or 100% of manufacturers' recommendations were tested. The results revealed a distinct peak separation of the different concentrations concerning the markers CD44 and CD49f where a positive signal was expected. Thus it was decided to use the total amount (100%) of antibody for each specific CSC marker in all further experiments.

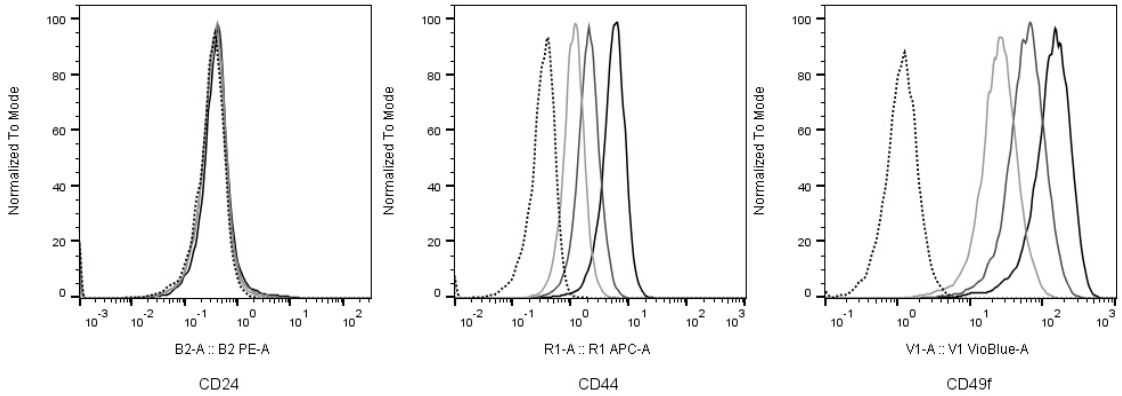

Figure 1. Antibody titration of breast cancer cell line MDA-MB-231. 25%, 50% and 100% amount of antibodies (CD24, CD44, CD49f) regarding the manufacturers' recommendations were tested. That is equivalent to an antibody working concentration of 20%, 10% and 5% (v/v) for CD24-AB, 0.5%, 0.25% and 0.125% (v/v) for CD44-AB, as well as 5%, 2.5% and 1.25% (v/v) for CD49f-AB. Light grey peak indicates 25%, grey peak 50% and dark grey peak 100% amount of antibody regarding the manufacturers' recommendations. The dotted peak indicates the untreated control sample.

4.2 Distribution of CSC marker

The CD44/CD24/CD49f surface expression profile was analyzed for the three breast cancer cell lines MDA-MB-231, MDA-MB-436 and MCF7 using flow cytometry. Deduced from the high frequency (> 90%) of $CD24^-/CD44^+$ cell subpopulation, the cell lines MDA-MB-231 and MDA-MB-436 exhibited extensive tumor-initiating properties (Figure 2). In contrast the MCF7 cell line was almost lacking of $CD24^-/CD44^+$ cell subpopulation (about 1%), suggesting the exhibition of much less tumor-initiating properties (Figure 2). Therefore the MCF7 cell line seemed to be an appropriate counterpart concerning the assignment of CSC properties.

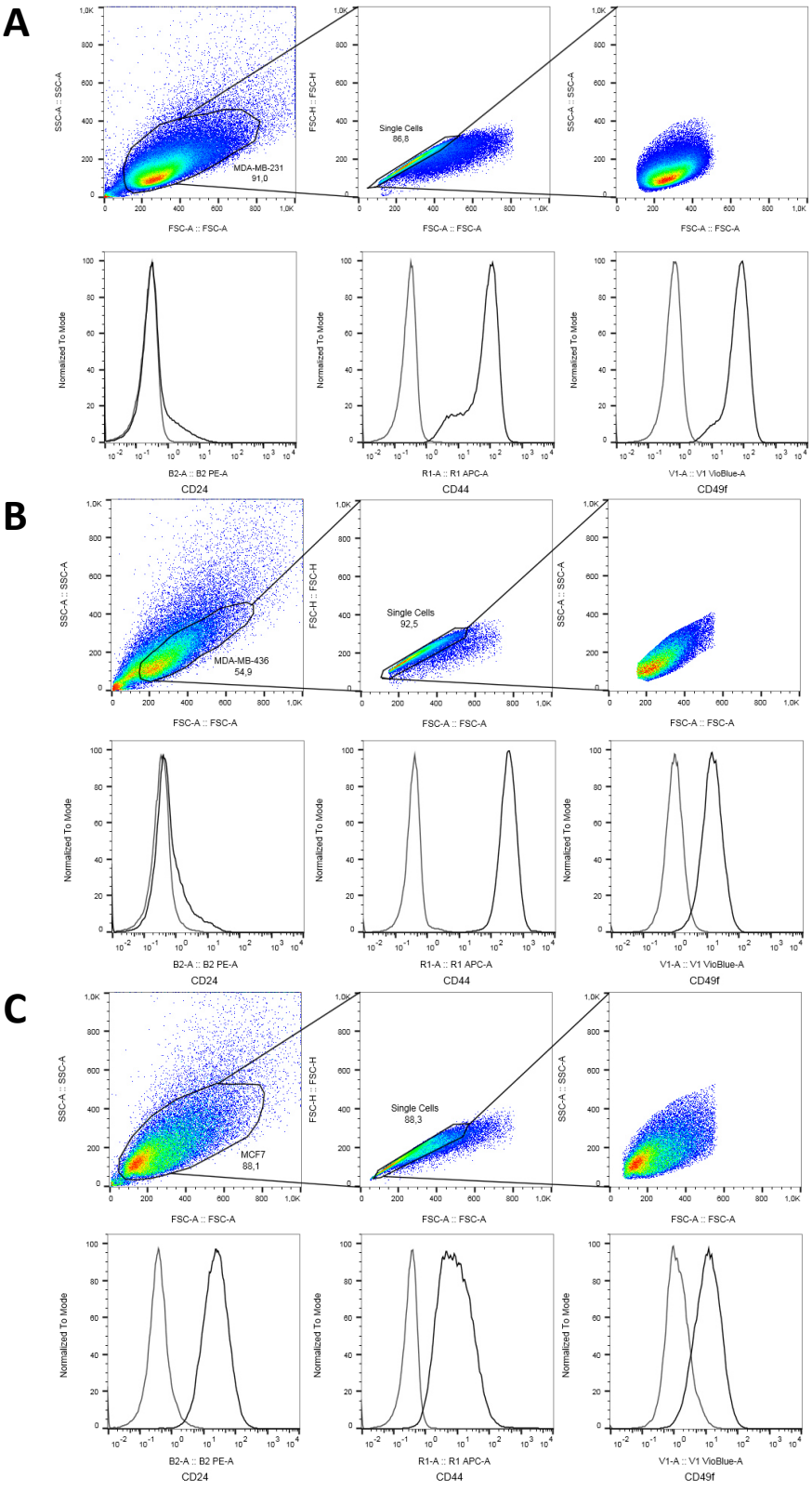

Figure 2. Expression analysis of CD24 (PE), CD44 (Alexa Fluor 647) and CD49f (Brilliant Violet 421) markers of MDA-MB-231 (A), MDA-MB-436 (B) and MCF7 (C) cell line by flow cytometry. First row: gating strategy applied for the evaluation of specified cell line. Second row: comparison of isotype control (grey peak) and normal primary antibody (black peak) for each marker for specified cell line.

The detailed evaluation of the CD24/CD44, CD24/CD49f as well as CD44/CD49f antigenic phenotype was accomplished with 2D dot-plots where the x-axes displayed the CD24 or CD44 and the y-axes displayed the CD44 or CD49f expression of the specified breast cancer cell line. The setting of thresholds for each marker resulted in deviation of the single gated cell populations into four quadrants (Q1-Q4, Q5-Q8 or Q9-Q12). Q1/Q5/Q9 equaled a $CD24^+/CD44^-$, $CD24^+/CD49f^-$ or $CD44^+/CD49f^-$, Q2/Q6/Q10 a $CD24^+/CD44^+$, $CD24^+/CD49f^+$ or $CD24^+/CD49f^+$, Q3/Q7/Q11 a $CD24^-/CD44^+$, $CD24^-/CD49f^+$ or $CD24^-/CD49f^-$ and Q4/Q8/Q12 a $CD24^-/CD44^-$, $CD24^-/CD49f^-$ or $CD24^-/CD49f^-$ surface marker specification of the cells within this quadrant.

Regarding the CD24/CD44 surface marker combination the following results were obtained: For MDA-MB-231 Q1($CD24^+/CD44^-$)=0.0%, Q2($CD24^+/CD44^+$)=6.6%, Q3($CD24^-/CD44^+$)=93.2% and Q4($CD24^-/CD44^-$)=0,1%; for MDA-MB-436 Q1($CD24^+/CD44^-$)=0.0%, Q2($CD24^+/CD44^+$)=7.7%, Q3($CD24^-/CD44^+$)=92.3% and Q4($CD24^-/CD44^-$)=0,1%; and for MCF7 Q1($CD24^+/CD44^-$)=0.4%, Q2($CD24^+/CD44^+$)=98.0%, Q3($CD24^-/CD44^+$)=1.3% and Q4($CD24^-/CD44^-$)=0,3%. These results are also summarized in a bar graph (Figure 3-B). The two major antigenic phenotypes in the single gated subpopulation of MDA-MB-231 as well as MDA-MB-436 cell line were $CD24^+/CD44^+$ with about 7% and $CD24^-/CD44^+$ with about 93% of the entire single gated cell population. In contrast the two major antigenic phenotypes in the single gated subpopulation of MCF7 cell line were $CD24^+/CD44^+$ with about 98% and $CD24^-/CD44^+$ with about 1% of the entire single gated cell population. In addition images of the three cell lines were taken at 10x magnification to observe potential relationships between antigenic phenotype and cell morphology (Figure 3-C). In this way a correlation between CD24 prevalent antigenic phenotype and cell morphology was identified. A luminal-like appearance for prevalent $CD24^+$ cell line MCF7 and a basal/mesenchymal appearance for mainly $CD24^-$ cell lines MDA-MB-436 and MDA-MB-231 was observed (Figure 3).

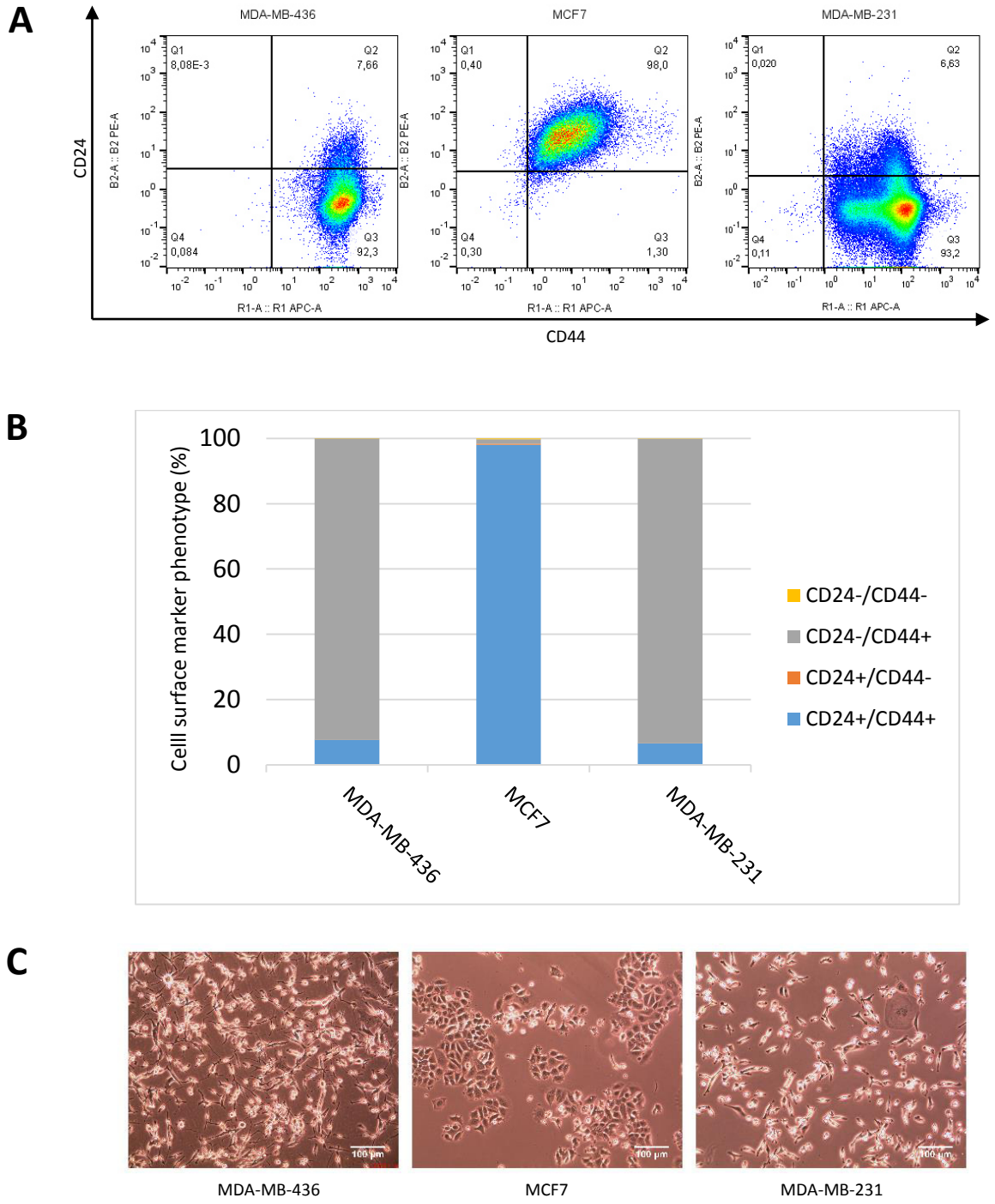

Figure 3. Evaluation of CD24/CD44 phenotype in MDA-MB-436, MCF7 and MDA-MB-231 human breast cancer cell lines. A) The expression of CD24 and CD44 markers was tested by flow cytometry for each cell line. The percentage of each population within the gated single cells is shown. B) Summarized results are represented in bar graph. C) Images taken at 10x magnification (Motic AE31 Series, Moticam 3.0MP). Scale bar is 100 µm. Luminal-like cell morphology exhibited by MCF7 human breast cancer cell line; basal/mesenchymal cell morphology exhibited by MDA-MB-231 and MDA-MB-436 human breast cancer cell lines.

Concerning the CD24/CD49f surface marker combination the following results were obtained: For MDA-MB-436 Q5($CD24^+/CD49f^-$)=0.1%, Q6($CD24^+/CD49f^+$)=8.0%, Q7($CD24^-/CD49f^+$)=88.0% and Q8($CD24^-/CD49f^-$)=3.9%; for MDA-MB-231 Q5($CD24^+/CD49f^-$)=0.0%, Q6($CD24^+/CD49f^+$)=6.6%, Q7($CD24^-/CD49f^+$)=93.2% and Q8($CD24^-/CD49f^-$)=0,1%; and for MCF7 Q5($CD24^+/CD49f^-$)=28.2%, Q6($CD24^+/CD49f^+$)=70.2%, Q7($CD24^-/CD49f^+$)=0.3% and Q8($CD24^-/CD49f^-$)=1.3%. These results are also summarized in a bar graph (Figure 4-B). With respect to these results the two major antigenic phenotypes in the single gated subpopulation of MDA-MB-231 as well as MDA-MB-436 cell line were $CD24^+/CD49f^+$ and $CD24^-/CD49f^+$. In contrast the two major antigenic phenotypes in the single gated subpopulation of MCF7 cell line were $CD24^+/CD49f^+$ with about 70% and $CD24^+/CD49f^-$ with about 28% of the entire single gated cell population. So, the antigenic phenotypes $CD24^-/CD49f^+$ and $CD24^-/CD44^+$ showed similar frequencies (ca. 90%) in the single gated cell population of MDA-MB-231 and MDA-MB-436 breast cancer cell lines (Figure 3,4). For the MCF7 cell line the surface marker exchange from CD44 to CD49f revealed changes in the evaluation of the abundance of the antigenic phenotypes. $CD24^+/CD44^+$ was the major antigenic phenotype with 98%, whereas $CD24^+/CD49f^+$ showed less abundance of 70%, followed by $CD24^+/CD49f^-$ with 28% of single gated cell population (Figure 3,4,5).

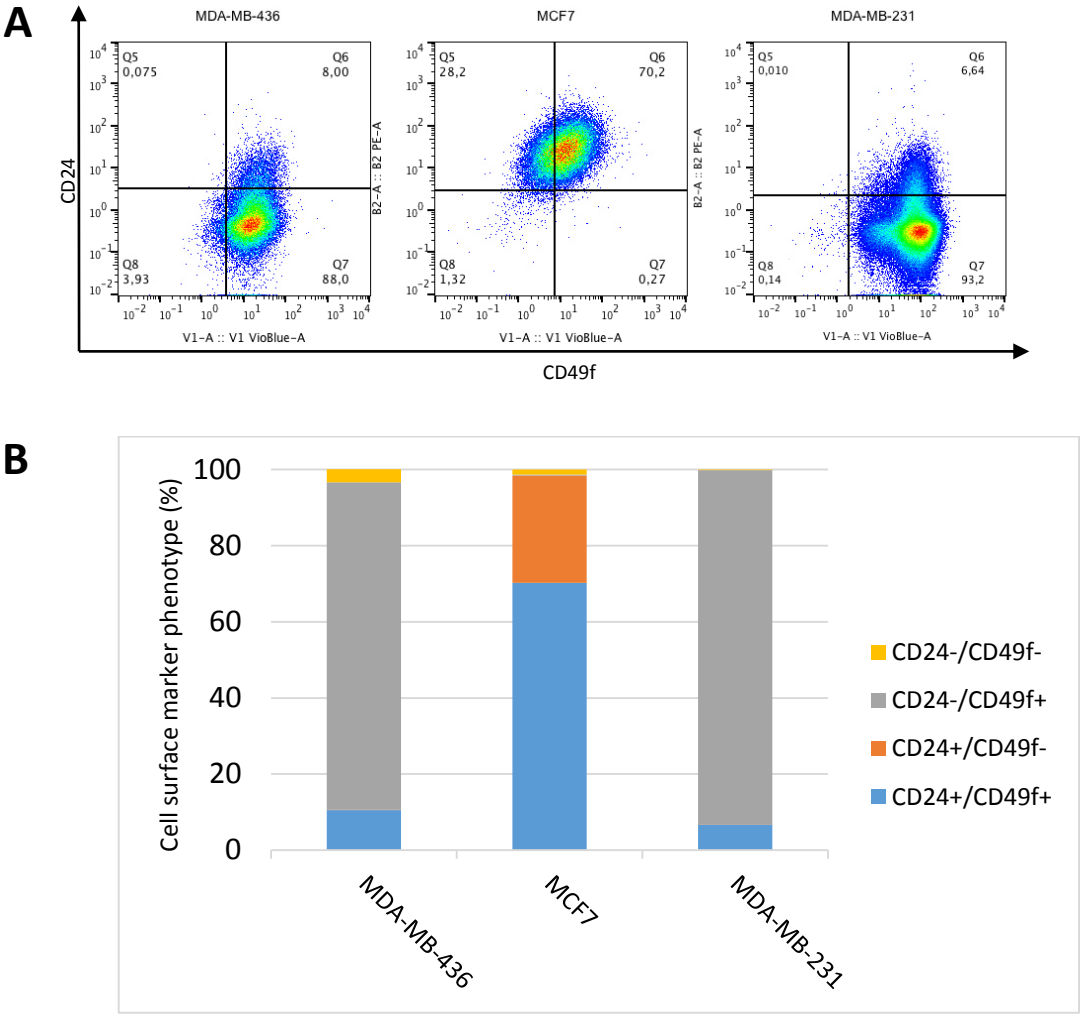

Figure 4. Evaluation of CD24/CD49f phenotype in MDA-MB-436, MCF7 and MDA-MB-231 human breast cancer cell lines. The expression of CD49f and CD24 markers was tested by flow cytometry for each cell line. A) The percentage of each population within the gated single cells is shown. B) Summarized results are represented in bar graph.

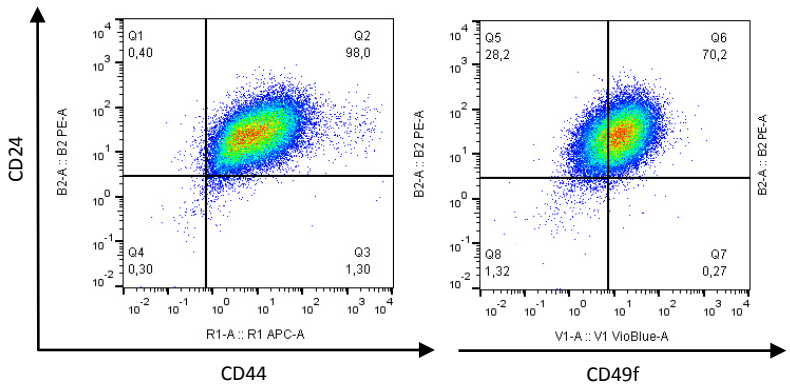

Figure 5. Influence of surface marker exchange from CD44 to CD49f in MCF7 cell line. The percentage of each population within the gated single cells is shown.

Concerning the CD44/CD49f surface marker combination the following results were obtained: For MDA-MB-436 Q9($CD44^+/CD49f^-$)=3.6%, Q10($CD44^+/CD49f^+$)=96.3%, Q11($CD44^-/CD49f^+$)=0.0% and Q12($CD44^-/CD49f^-$)=0.1%; for MDA-MB-231 Q9($CD44^+/CD49f^-$)=0.1%, Q10($CD44^+/CD49f^+$)=99.7%, Q11($CD44^-/CD49f^+$)=0.2% and Q12($CD44^-/CD49f^-$)=0.1%; and for MCF7 Q9($CD44^+/CD49f^-$)=29.1%, Q10($CD44^+/CD49f^+$)=70.0%, Q11($CD44^-/CD49f^+$)=0.2% and Q12($CD44^-/CD49f^-$)=0.8%. With respect to these results the major antigenic phenotype in the single gated subpopulation of MDA-MB-231 as well as MDA-MB-436 cell line was $CD44^+/CD49f^+$. In contrast the MCF7 cell line exhibited two major antigenic phenotypes, $CD44^+/CD49f^+$ with about 70% and $CD44^+/CD49f^-$ with about 29% of the entire single gated cell population. So, the antigenic phenotype $CD44^+/CD49f^+$ showed similar frequencies (ca. 90%) to $CD24^-/CD49f^+$ and $CD24^-/CD44^+$ in the single gated cell population of MDA-MB-231 and MDA-MB-436 breast cancer cell lines (Figure 3,4,6). Similar to CD24/CD49f, the surface marker combination CD44/CD49f revealed two major phenotypes of gated subpopulation in MCF7 cell line. $CD44^+/CD49f^+$ (70%) and $CD44^+/CD49f^-$ (29%) antigenic phenotype resembled the results for $CD24^+/CD49^+$ (70%) and $CD24^+/CD49f^-$ (28%) in MCF7 cell line (Figure 4,6).

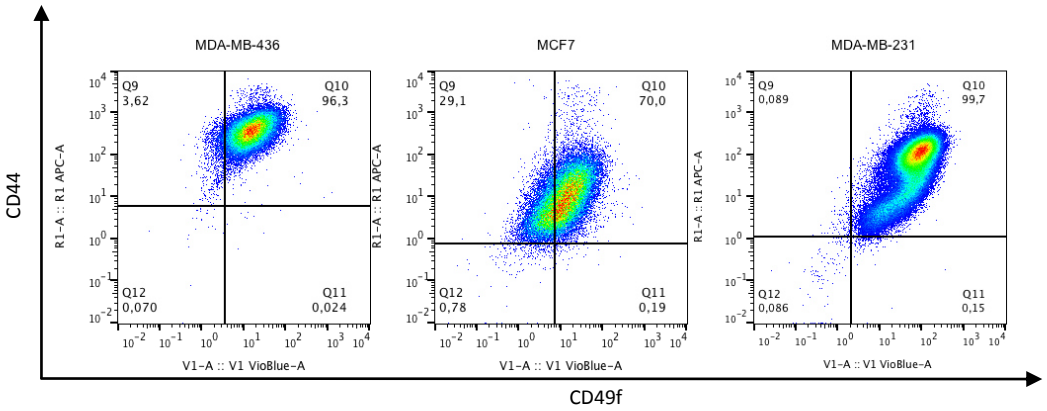

Figure 6. Evaluation of CD44/CD49f phenotype in MDA-MB-436, MCF7 and MDA-MB-231 human breast cancer cell lines. The expression of CD49f and CD44 markers was tested by flow cytometry for each cell line. The percentage of each population within the gated single cells is shown.

4.3 Salinomycin's dose-dependent effect on highly CSC marker expressing cells

In a next step, the cytotoxic effects of different concentrations of salinomycin on the breast cancer cell lines were tested. The experiment was combined with a flow-cytometry-based live-dead staining using propidium iodide (PI).

Salinomycin showed a dose-dependent cytotoxic effect on the human breast cancer cell lines with highly expressed CSC markers MDA-MB-436 and MDA-MB-231 (Figure 7). The higher the concentration of salinomycin was applied to these breast cancer cell lines, the higher was the number of PI positive cells detected. However, this dose-dependent tendency was not observed for the breast cancer cell line MCF7, which features less CSC properties as determined earlier. For the MCF7 cell line, most PI positive cells were measured for the solvent control (0.2% (v/v) DMSO) with more than 20%, followed by 1.0, 0.5 and 2.0 µM salinomycin application (Figure 7). Comparing the three cell lines, MCF7 indicated the highest percentage of PI positive cells for all tested conditions, followed by MDA-MB-231 and MDA-MB-436 cell line (Figure 7).

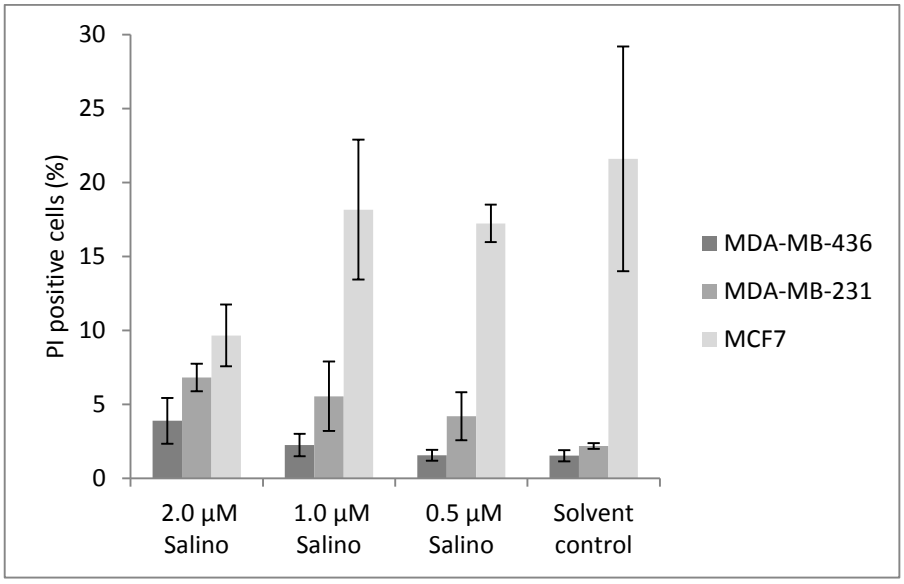

Figure 7. Percentage of PI positive breast cancer cells after 72 h of salinomycin treatment. The breast cancer cell lines MDA-MB-231, MDA-MB-436 and MCF7 were treated with different concentrations of salinomycin (abbreviated as salino), as well as a solvent control (0.2% (v/v) DMSO). After 72 h of treatment a live-dead staining with PI was measured by flow cytometry. Bars represent mean values. Error bars represent the standard deviation (SD).

4.4 Salinomycin does not affect the CSC marker profile

The next experiment was conducted to investigate the effects of salinomycin on the antigenic phenotype of breast cancer cell lines. For this experiment the mesenchymal breast cancer cell line MDA-MB-231 which indicated a high degree of CSC properties (Chapter 4.2), and the luminal breast cancer cell line MCF7 as a counterpart, was used. Furthermore the chemotherapeutic daunorubicin was tested, and the combination of salinomycin and daunorubicin without CSC marker determination. The applied concentrations were 0.5 µM salinomycin/daunorubicin, 1.0 µM salinomycin/daunorubicin, 2.0 µM salinomycin/daunorubicin and 1.0 µM salinomycin-daunorubicin.

Images taken after 4 days of treatment revealed the increase of cytotoxic effect of salinomycin with higher concentrations. In comparison with the chemotherapeutic daunorubicin and the combination of salinomycin with daunorubicin, salinomycin alone appeared to be less cytotoxic with regard to the images (Figure 8). Comparing the breast

cancer cell lines MCF7 and MDA-MB-231 no differences occurred concerning cytotoxic effects of the drugs on the basis of the images regardless of whether before or after the recovery phase (Figure 8).

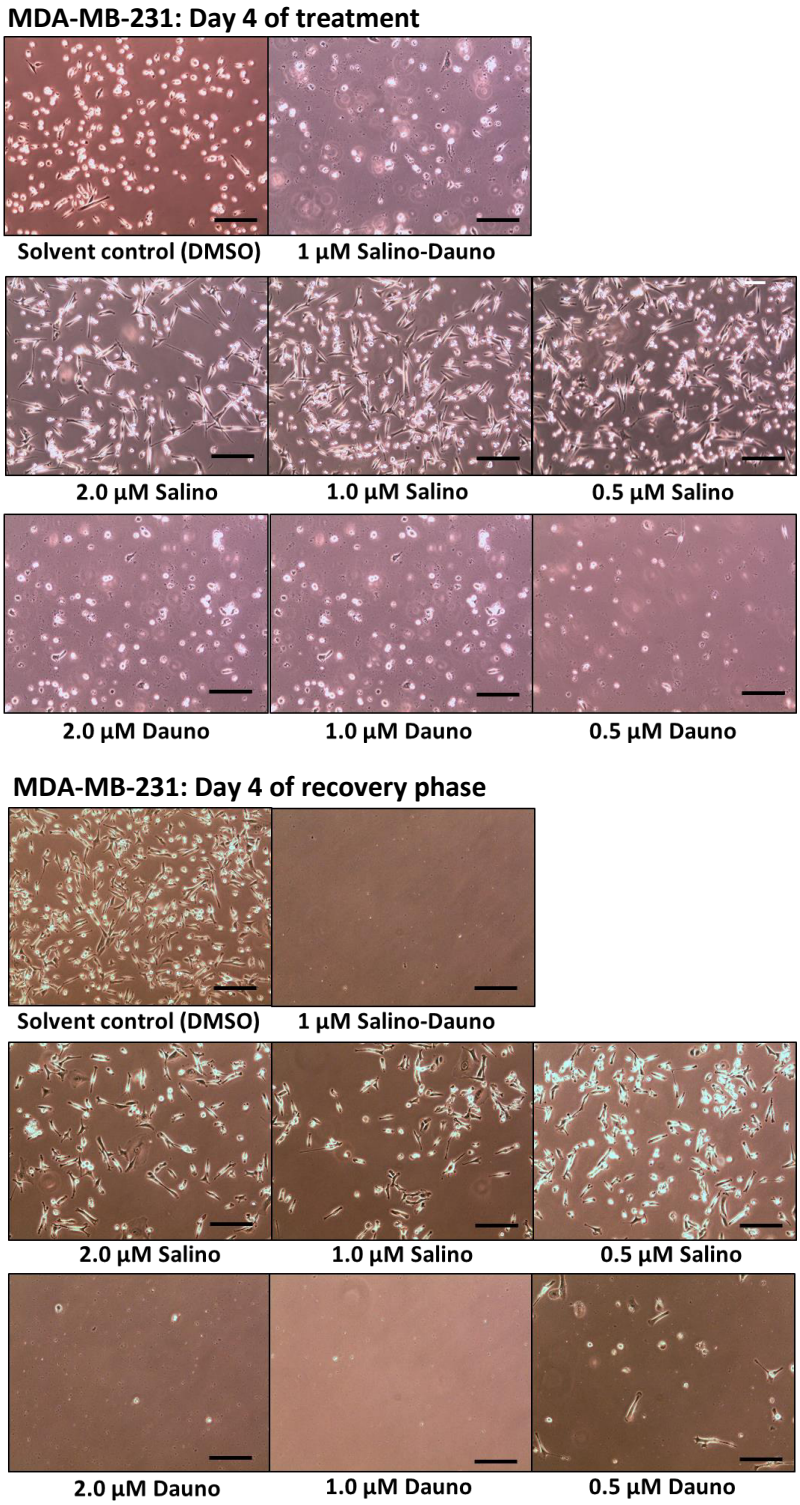

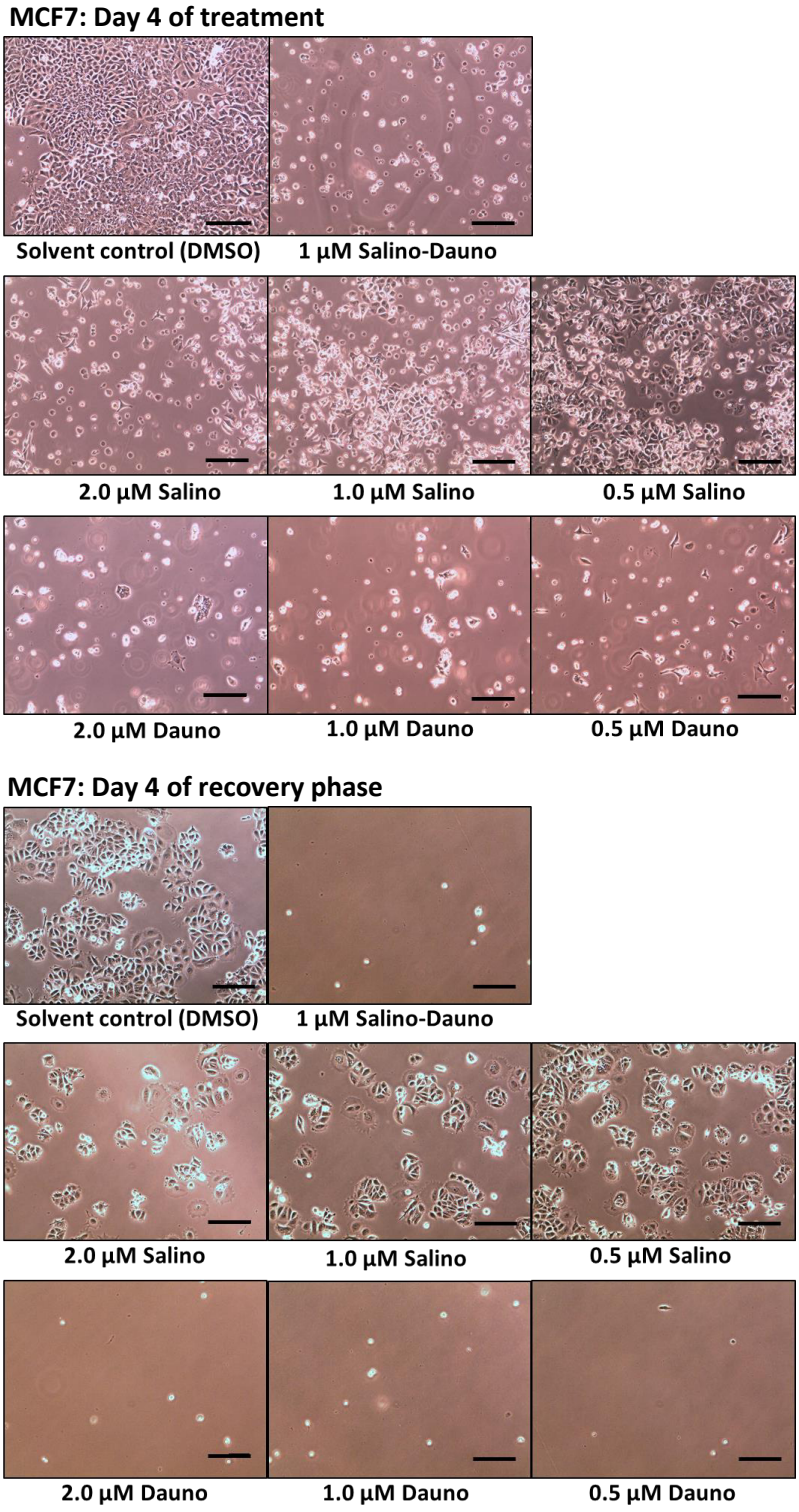

Figure 8. MCF7 or MDA-MB-231 breast cancer cells after 4 days of specified treatment and after 4 days of recovery phase. The cells were first treated with specified doses of daunorubicin (abbreviated as dauno) and salinomycin (abbreviated as salino) for 4 days, passaged in adjusted ratio and then allowed to recover for 4 days. The medium was renewed every day during the recovery phase. Images were taken at 10x magnification (Motic AE31 Series, Moticam 3.0MP). Scale bar is 200 µm.

For the CSC marker evaluation of the pre-treated cells the data was analyzed in the same manner as in Chapter 4.2 yielding dot-plots divided into four quadrants (Q1-Q4 or Q5-Q8). The results of the CSC evaluation after 4 days of recovery revealed that salinomycin did not induce a shift of the population from $CD24^-/CD44^+$ antigenic phenotype towards other antigenic phenotypes in MDA-MB-231 cell line. The cell line MCF7 was also not affected by salinomycin with respect to the antigenic phenotype. MCF7 cell population remained in $CD24^+/CD44^+$ antigenic phenotype (Figure 9). Analyzing of the CD24/CD49f antigenic phenotype showed similar results, meaning no shift of the cell populations for neither MCF7 nor MDA-MB-231 cell line (Figure 10). These findings were reflected in the images taken after 4 days of recovery, meaning that no phenotypic differences between the conditions were observed for both breast cancer cell lines. Salinomycin treated MCF7 or MDA-MB-231 breast cancer cells were able to recover well, whereas daunorubicin or daunorubicin-salinomycin treated cells were almost eliminated after 4 days of recovery phase (Figure 8).

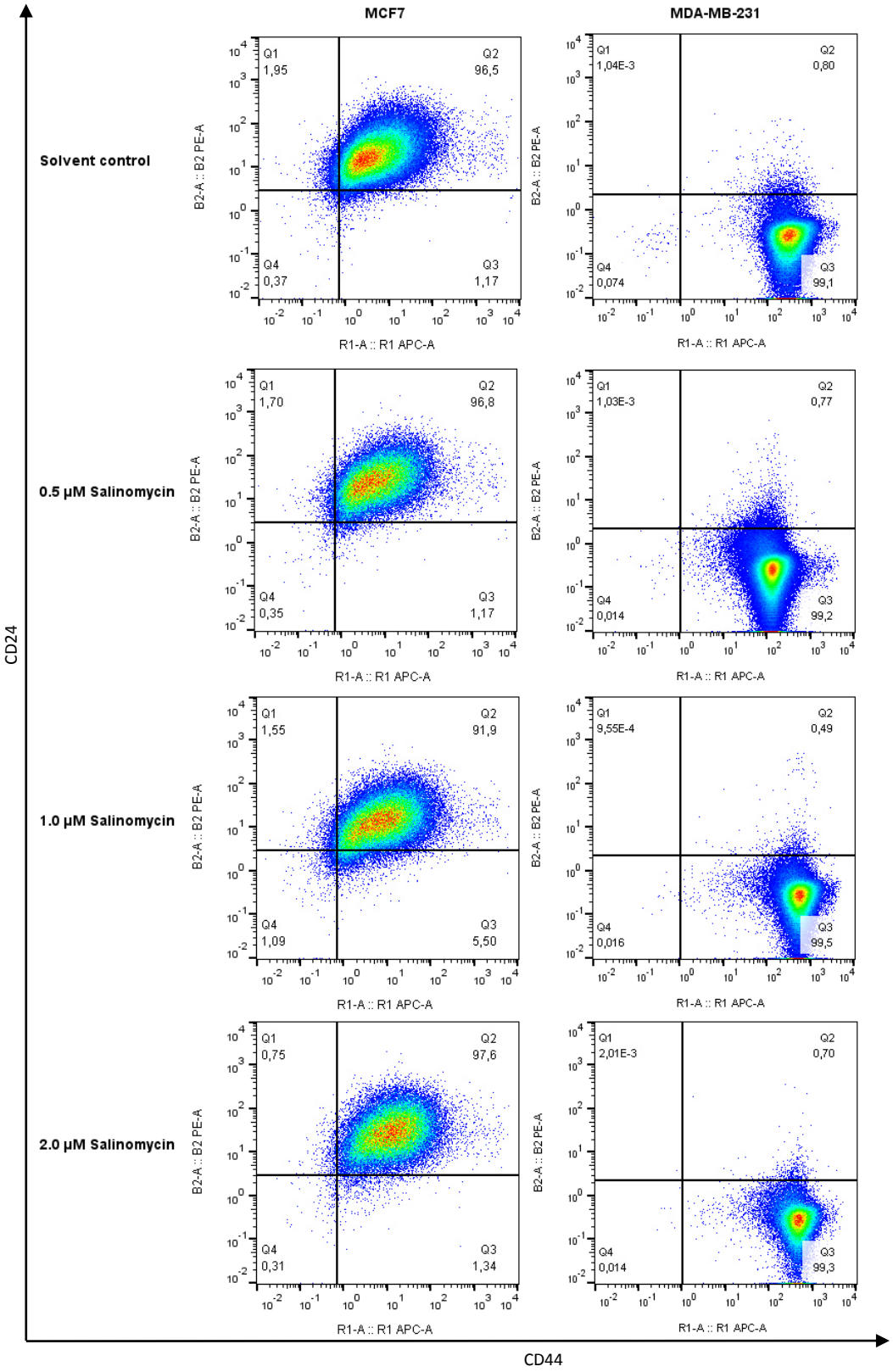

Figure 9. Influence of salinomycin treatment on CD24/CD44 antigenic phenotype of MCF7 and MDA-MB-231 breast cancer cell lines. The expression of CD24 and CD44 markers upon salinomycin treatment was tested by flow cytometry for each cell line. The cells were treated at the specified doses for 4 days, and then allowed to recover in the absence of treatment for 4 days. The percentage of each population is shown.

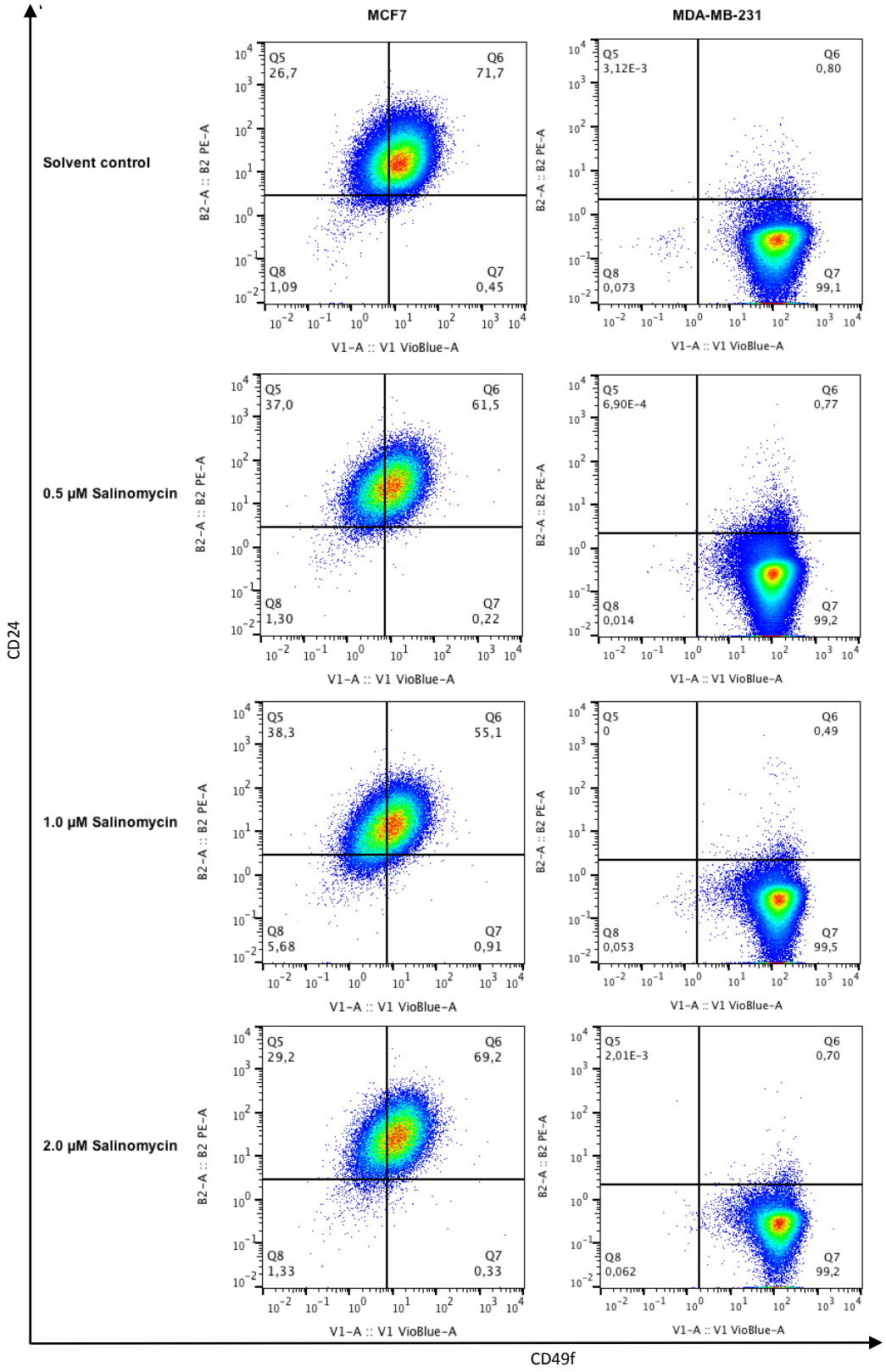

Figure 10. Influence of salinomycin treatment on CD24/CD49f antigenic phenotype of MCF7 and MDA-MB-231 breast cancer cell lines. The expression of CD24 and CD49f markers upon salinomycin treatment was tested by flow cytometry for each cell line. The cells were treated at the specified doses for 4 days, and then allowed to recover in the absence of treatment for 4 days. The percentage of each population is shown.

4.5 Soft agar colony formation assay

4.5.1 Optimization of soft agar colony formation assay

The soft agar colony formation assay was used to assess the stemness of the tested human breast cancer cell lines in vitro. Soft agar colony formation assay in 96-well plate format aiming at a high throughput strategy was attempted, but handling and evaluation were deemed unsatisfactory. The well shadow perturbed the quantitative evaluation of the images (Figure 11-A).

In the course of the optimization different endpoint evaluation procedures were tested. The cell viability dye thiazolyl blue tetrazolium bromide (MTT), the dye crystal violet, and the fluorescence dye Hoechst 34580 were compared. Formaldehyde fixation with subsequent crystal violet staining yielded satisfactorily stained spheroids which contrasted well (Figure 11-A,C). Once fixed and stained, plates could be stored in the fridge (4 °C) for months keeping its shape. The cell viability dye thiazolyl blue tetrazolium bromide (MTT) also achieved satisfactorily staining results (Figure 11-B,D), but failed since the combination with formaldehyde fixation did not work. The utilization of Hoechst 34580 did not achieve a sufficient contrast under fluorescence microscope owing to the background originating from agarose.

Therefore a prior formaldehyde fixation with subsequent crystal violet staining turned out to be the most convenient procedure. This evaluation procedure was maintained for further experiments in 6-well plate format. ImageJ® was used to quantify the clearly visible spheroids manually (Figure 12).

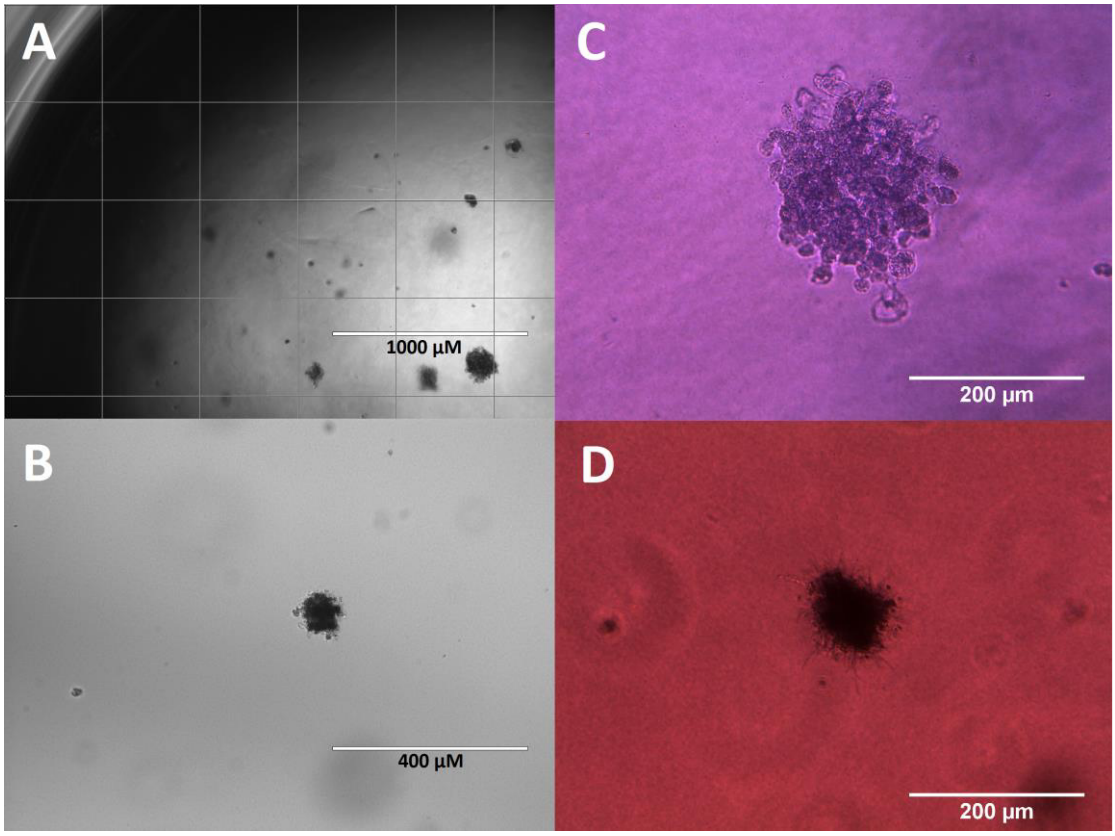

Figure 11. Endpoint evaluation tests of soft agar colony formation assay in 96-well plate format. 1000 MDA-MB-436 breast cancer cells per well were initially seeded. A, C) Formaldehyde fixed and crystal violet (CV) stained well. A) Well shadow perturbs the quantitative analysis of the spheroids. 4x magnification (EVOS FL Thermo Fisher Scientific®, Waltham, MA, USA). C) 20x magnified CV stained spheroid (Motic AE31 Series, Moticam 3.0MP). B, D) Thiazolyl blue tetrazolium bromide (MTT) stained spheroid without formaldehyde fixation. B) 10x magnification with EVOS FL. D) 20x magnification (Motic AE31 Series, Moticam 3.0MP).

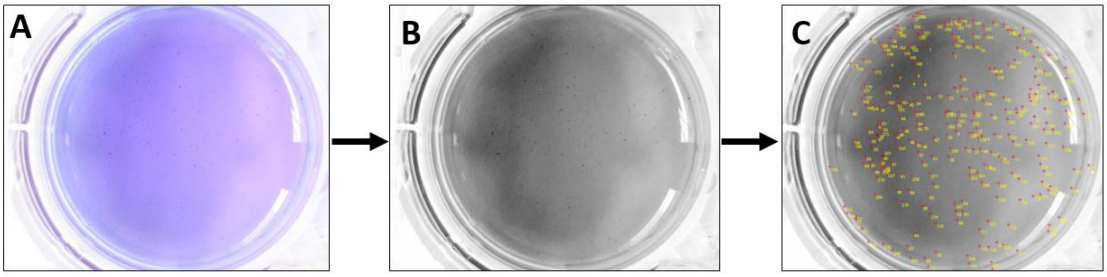

Figure 12. Evaluation approach for soft agar colony formation assay. A) Wells were fixed (formaldehyde) and stained (crystal violet). B) To simplify counting Images were converted into 16-bit format using ImageJ®. C) Spheroids were counted manually with the help of multipointer tool in ImageJ®.

4.5.2 High variation of spheroid number and size

The soft agar colony formation assay for the three breast cancer cell lines revealed a high variation in spheroid size and number. After 21 days of growing the biggest spheroids were obtained for the MCF7 cell line with about 29 x 10^3 µm^2 followed by the MDA-MB-231 cell line with about 18 x 10^3 µm^2 and the MDA-MB-436 cell line with about 9 x 10^3 µm^2 (Figure 13). Mean spheroid numbers per well were 271 for MCF7, 64 for MDA-MB-436 and 40 for MDA-MB-231 cell line (Figure 13). In summary, MCF7 cell line exhibited enhanced growth ability of spheroids in comparison with the other cell lines MDA-MB-231 and MDA-MB-436, reflected in higher spheroid numbers and sizes.

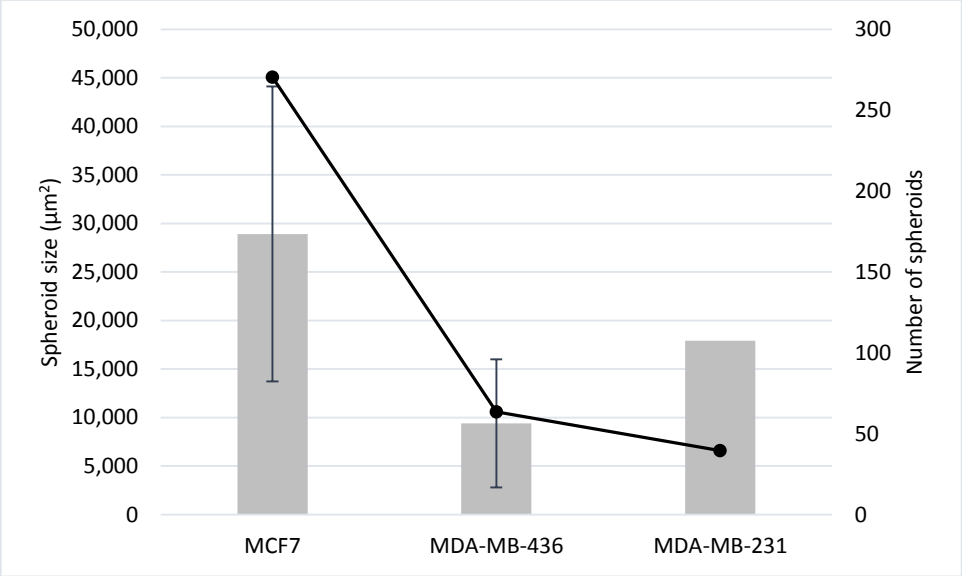

Figure 13. Evaluation of soft agar colony formation assay after 21 days. The initial cell number was 5000 cells per well. The wells were fixed and stained, then photos were taken with a camera. 4x magnification (Motic AE31 Series, Moticam 3.0MP) was applied to determine the spheroid size. ImageJ® was used to count the spheroids. Bars represent the mean spheroid size, line indicates the number of spheroids counted. Error bars represent the standard deviation (SD) of the spheroid size. SD was calculated for samples with n ≥ 3.

The remaining viable cells after chemotherapeutic treatment (Chapter 4.4) were seeded into soft agar to test their ability to grow in non-adherent environment. Based on the high capability of CSCs to grow in non-adherent environment, it was expected that cell populations treated with the CSC targeting drug salinomycin would exhibit less ability to form spheroids. For the pre-treated MCF7 as well as the MDA-MB-231 cell lines a high variation for spheroid numbers and sizes of the different conditions was obtained (Figure 13). Therefore the pre-treated cells indicated no dose-dependent correlation between the specific salinomycin treatment and the spheroid number or size. Remaining cells after daunorubicin or salinomycin-daunorubicin treatment also showed spheroid growth in soft agar (data not shown). Spheroid numbers and sizes of these spheroids were similar to those of the salinomycin treatments.

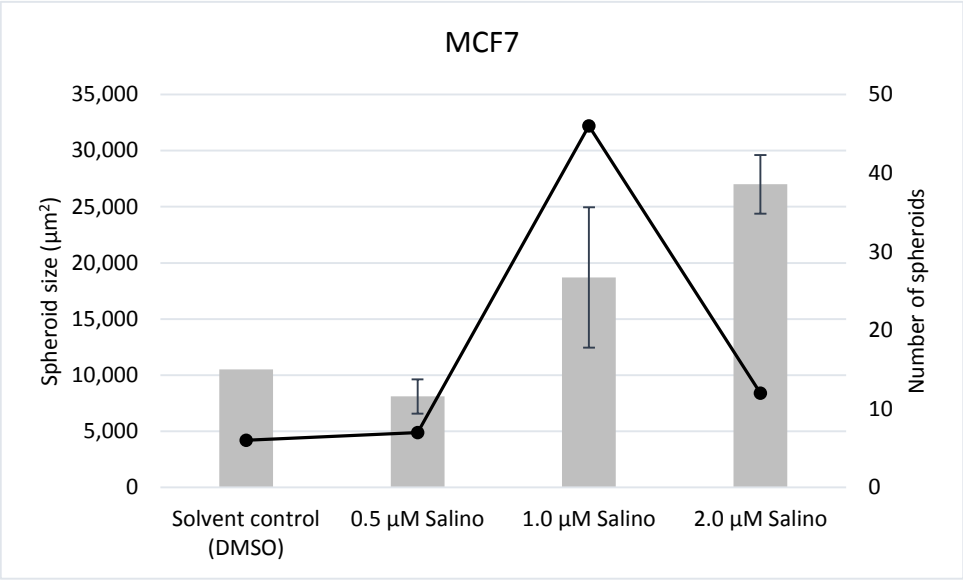

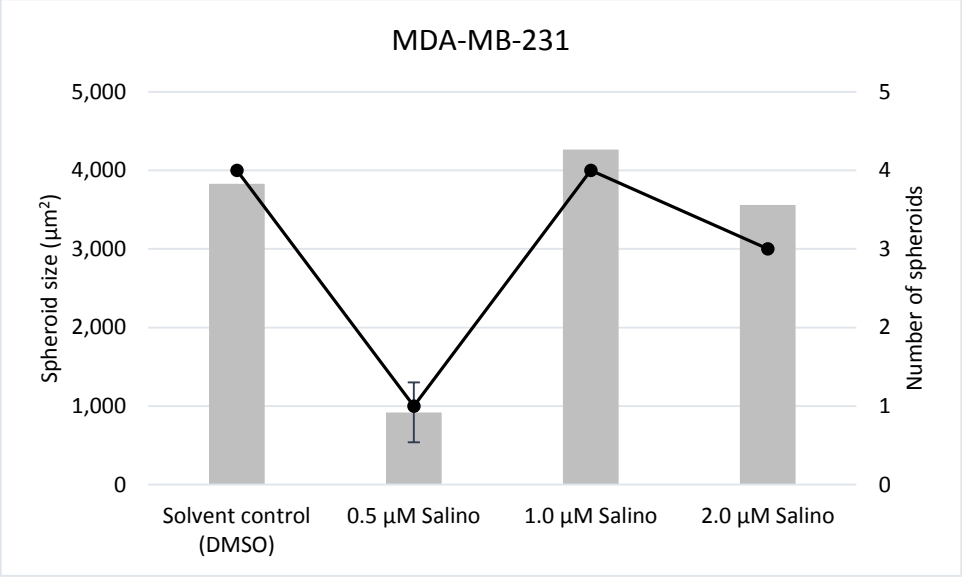

Figure 14. Soft agar colony formation assay of pre-treated cells. 5000 cells (MCF7 or MDA-MB-231) per well were seeded into soft agar. Prior cells were pre-treated with specified doses for 4 days, then allowed to recover for 4 days in the absence of any treatment. After fixation and staining on day 20, photos were taken with a camera. 4x magnification was applied to determine the size of the spheroids (Motic AE31 Series, Moticam 3.0MP). ImageJ® was used to count the spheroids. Bars indicate the mean spheroid size, line indicates the number of spheroids counted. For 0.5 µM salinomycin (MCF7) only one spheroid was counted which is not enough to obtain statistically significant results. Error bars represent the standard deviation (SD) of the spheroid size. SD was calculated for samples with $n \geq 3$.

In about half of the wells, problems with the two soft agar layers occurred. In the assay without treatment the distinction between top- and bottom layer disappeared as the agar turned into a more liquid state. Moreover cells sank to the bottom of the well exhibiting 2D phenotype and massive growing in the assay with treatment. Subsequently, statistical evaluation was not possible. In an optimization experiment, the plate was put into the fridge (4 °C) for 45 minutes after pouring the bottom layer, alleviating the problem of agar liquefaction.

4.6 The methyl cellulose assay for faster production of multicellular aggregates

The methyl cellulose assay was introduced to establish a faster method for obtaining multicellular aggregates than with the soft agar colony formation assay. Thousands of cells are deposited in each U-bottom well, sink down and attach each other to form a multicellular aggregate. This multicellular aggregates can then be left to grow until isolation. As such, this method represents a fast way to produce multicellular aggregates. Additionally, methyl cellulose represents a quasi-liquid system facilitating easy spheroid retrieval, contrary to approaches including matrigel and soft agar. As a result, the methyl cellulose assay can provide easier accessible multicellular aggregates in a more rapid fashion, ideal for testing novel downstream methods such as histological cryosectioning.

In an optimization experiment, the initial cell number of breast cancer cell line MDA-MB-231 was varied and images were taken after 24 hours of growing (Figure 15).

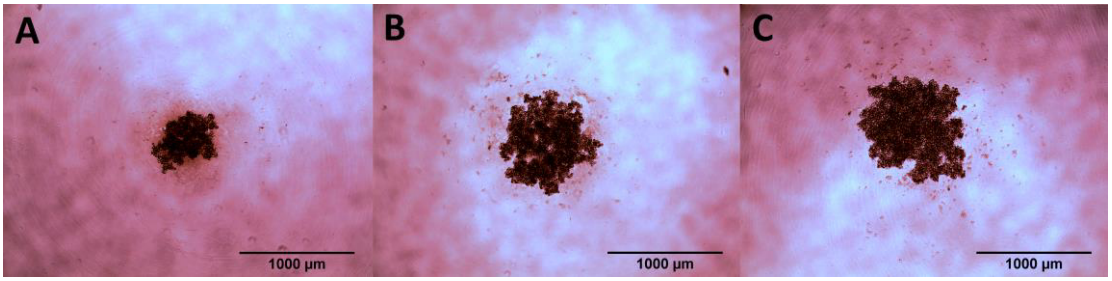

Figure 15. Multicellular aggregates after 24 h of growing obtained by the methyl cellulose assay. Human breast cancer cell line MDA-MB-231 was used. A) Initial cell number was 1000 cells per well. Size measured was 18.9 x 10^3 µm^2. B) Initial cell number was 2500 cells per well. Size measured was 48.9 x 10^3 µm^2. C) Initial cell number was 4167 cells per well. Size measured was 61.1 x 10^3 µm^2. All images were taken at 4x magnification (Motic AE31 Series, Moticam 3.0MP). Spheroid sizes were determined in ImageJ®.

5. Discussion

In this work we established a method for the antigenic phenotype determination of breast cancer cell lines with focus on CSC markers. In principle the method was based on primary fluorophore conjugated antibodies facilitating a flow cytometry-based measurement. Our optimized procedure fulfilled our aims to establish a convenient, time-efficient, antibody-amount-saving and reproducible method which can be carried out in a 96-well plate format. The nature of the primary antibodies allowed a parallel application, thus contributing to time-efficiency. We concentrated on the CD24 (PE), CD44 (Alexa Fluor 647) and CD49f (Brilliant Violet 421) markers. CD24 and CD44 markers have been demonstrated to be the most important CSC markers in the last years (Al-Hajj et al., 2003). CD49f marker is in comparison a relatively unknown marker for CSCs (Cariati et al., 2008).

Using our optimized antibody staining method we started with the characterization of the human breast cancer cell lines MDA–MB-231, MDA-MB-436 and MCF7. Mainly $CD24^-/CD44^+$ subpopulation (>90%) of cells was detected for the two basal/mesenchymal cell lines MDA-MB-231 and MDA-MB-436. In contrast the luminal-like MCF7 cell line exhibited the $CD24^+/CD44^+$ antigenic phenotype (98%) most prevalently. With regard to $CD24^-/CD44^+$

antigenic phenotype our results resembled those found in the literature (Figure 16, Fillmore and Kuperwasser, 2008; Keller et al., 2010; Manuel Iglesias et al., 2013).

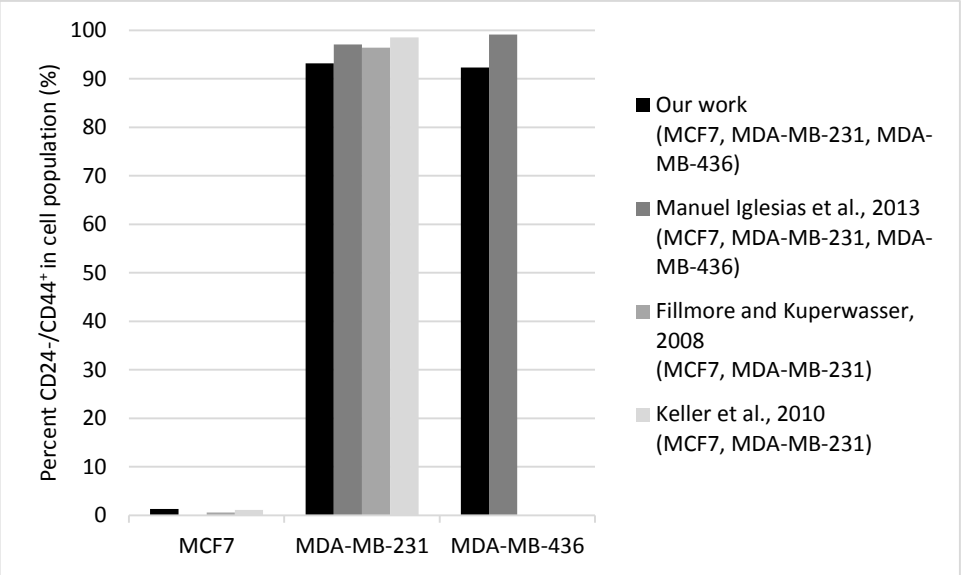

Figure 16. Accordance of CD24$^-$/CD44$^+$ marker expression with literature. The expression of CD24 and CD44 markers was tested by flow cytometry for each cell line. Bars represent percentage of CD24$^-$/CD44$^+$ subpopulation within single gated cell population. Black bars represent our results, grey bars the findings in the literature.

It was demonstrated that the additional CD49f marker was similarly frequent (>90%) within the single gated cell population as the CD44 marker in the two basal/mesenchymal cell lines MDA-MB-231 and MDA-MB-436. However in the MCF7 cell line the CD24$^+$/CD49f$^+$ antigenic phenotype was less abundant (70%) than the CD24$^+$/CD44$^+$ antigenic phenotype (98%). The distribution of the two main cell subpopulations in the MCF7 cell line, CD24$^+$/CD49f$^+$ (ca. 70%) and CD24$^+$/CD49f$^-$ (ca. 28%), resembled the findings in the literature of about 64% CD24$^+$/CD49f$^+$ and 34% CD24$^+$/CD49f$^-$ cell population (Keller et al., 2010). For the surface marker combination CD44/CD49f mainly CD44$^+$/CD49f$^+$ subpopulation (>95%) of cells was detected for the two basal/mesenchymal cell lines MDA-MB-231 and MDA-MB-436. In the MCF7 cell line CD44/CD49f surface marker combination revealed the two main cell populations of 70% CD44$^+$/CD49f$^+$ and 29% CD44$^+$/CD49f$^-$. These results were similar to those of the CD24/CD49f surface marker combination.

The CD24 prevalent antigenic phenotype exhibited a correlation with cell morphology. A luminal-like appearance for prevalent $CD24^+$ cell line MCF7 and a basal/mesenchymal appearance for prevalent $CD24^-$ cell lines MDA-MB-436 and MDA-MB-231 was observed, which also has been documented in literature (Fillmore and Kuperwasser, 2008). The high abundance of $CD24^-/CD44^+$ surface marker profile (>90%) in the MDA-MB-231 and MDA-MB-436 breast cancer cell lines was assumed to assign CSC properties to these cell lines. However, according to selected literature these marker combination is not sufficient to determine CSC subpopulation within cell lines. The additional utilization of the ESA (epithelial-specific antigen) marker has been documented to more specifically detail the CSC subpopulation, resulting in about 2% of $CD24^-/CD44^+/ESA^+$ subpopulation in MDA-MB-231 cell line (Fillmore and Kuperwasser, 2008).

We performed a salinomycin treatment to compare the effects of this CSC targeting drug on the cell lines MCF7, MDA-MB-231 and MDA-MB-436. In addition we treated the cell lines with the chemotherapeutic drug daunorubicin and the combination of salinomycin with daunorubicin. A PI-based live-dead staining after 72 h of treatment detected that salinomycin eliminates the basal/mesenchymal cell lines MDA-MB-231 and MDA-MB-436 in a dose-dependent manner. For the luminal-like MCF7 cell line these dose-dependent effects were not observed, reflected in the highest value for PI positive cells of more than 20% for the solvent control. The evaluation after 72 h of treatment represented a snapshot, where the current percentage of PI positive cells was analyzed. Using this evaluation method, the recording of growth curves was omitted. The above-mentioned curious result for the MCF7 cell line could be defective. The finding that salinomycin (together with 0.05%-0.2% (v/v) DMSO) eradicated cell lines with high amount of CSC subpopulation in a dose-dependent manner, underlined the presumed CSC killing ability of salinomycin (Gupta et al., 2009). However, images of treated cells revealed similar dose-dependent cytotoxic effects for MCF7 and MDA-MB-231 cell line. Therefore the applicability of the PI-based live-dead staining on MCF7 cells will have to be confirmed in further experiments. The different cell morphology of MCF7 cells could cause difficulties in this PI-based approach. Considering the images after treatment, daunorubicin and the combination of salinomycin with daunorubicin eliminated more of the cells than salinomycin alone. This finding underlines the tenor in the literature to combine salinomycin with conventional anticancer drugs in order to enhance the ability to

effectively treat cancer (Naujokat and Steinhart, 2012). Daunorubicin was able to eradicate almost all MDA-MB-231 cells, with strongest cytotoxicity for the two highest applied concentrations of 1.0 and 2.0 µM with regard to the images of the treated cells. In accordance with our results, the daunorubicin-related drug doxorubicin has been documented to induce apoptosis in the MDA-MB-231 cell line at similar concentrations of about 1.5 µM (Ghebeh et al., 2010).

In our main experiment we proved whether the treatment with salinomycin has an impact on the CD24/CD44/CD49f antigenic profile of the luminal-like MCF7 cell line and the basal/mesenchymal MDA-MB-231 cell line. Furthermore we tested the ability of this pre-treated cells to form spheroids in non-adherent environment using the soft agar colony formation assay. Based on one hand that salinomycin represents a CSC targeting drug and on the other hand that CSCs are able to grow in soft agar, it was expected that salinomycin treated cells exhibit less ability to grow in soft agar. The results of the antigenic phenotype evaluation for CD24, CD44 and CD49f markers did not show any changes forced by the salinomycin treatment in MDA-MB-231 or MCF7 cells. Therefore the finding of Gupta and co-workers, that salinomycin decreased the proportion of $CD44^{+}/CD24^{-}$ breast cancer cells by 20-fold relative to vehicle control in SUM159 or HMLER (human mammary epithelial cells) cells, was not reproduced for our cell lines (Gupta et al., 2009). In the soft agar colony formation assay of the pre-treated MCF7 and MDA-MB-231 cells any correlation between the spheroid formation (quantity, size) and the applied treatment was missing. Related studies showed that salinomycin treatment induced a 10-fold decrease in the number of spheroids for other cell lines (Gupta et al., 2009). These results have been detected by a different tumor-sphere assay using ultralow attachment plates (Dontu, 2003). Further experiments in the same experimental layout will have to be carried out in order to confirm our results for the cell lines MDA-MB-231 and MCF7. Problems with agarose liquefaction complicated the evaluation of the soft agar colony formation assay. In an optimization experiment we managed to solve the problem. Our optimized method can be used for further experiments.

The methyl cellulose assay is a fast method to obtain multicellular aggregates (Bilandzic and Stenvers, 2014). Therefore we attempted an optimization experiment for this assay where we tested different MDA-MB-231 cell numbers. The generation of multicellular aggregates

was successful. Based on this method multicellular aggregates could be isolated, enabling easy generation of spheroids for testing of novel methods for spheroid analysis.

In summary we were able to set up appropriate versatile combination of methods to analyze breast cancer cell lines for their CSC properties including antigenic phenotype, effects on drug treatment and the ability to form spheroids in non-adherent environment. Our work provides the basis for further experiments on the clinically relevant subpopulation of CSCs within breast cancer cell lines.

6. Appendix

6.1 Abstract

Cancer stem cells (CSCs) represent an important subclass of neoplastic cells with high clinical relevance. In this work we established methods for time-efficient and reproducible analysis of CSC properties, namely a cell surface marker based flow-cytometry based identification method and a soft agar colony formation assay. The three surface marker CD24, CD44 and CD49f were selected. We focused on the basal/mesenchymal human breast cancer cell lines MDA-MB-231 and MDA-MB-436, as well as the luminal-like human breast cancer cell line MCF7. Using the optimized evaluation method, the cell lines were characterized for their CD24/CD44/CD49f antigenic surface profile. The characterization revealed that the two basal/mesenchymal-like cell lines MDA-MB-231 and MDA-MB-436 predominantly exhibited $CD24^-/CD44^+/CD49f^+$ antigenic phenotype, whereas the luminal-like cell line MCF7 exhibited the $CD24^+/CD44^+/CD49f^+$ antigenic phenotype most frequently. In a next step, we utilized the promising CSC targeting drug salinomycin. We tested the cytotoxic effects of salinomycin and the chemotherapeutic daunorubicin on the three cell lines. Using a live-dead staining based approach coupled with flow cytometry we found that salinomycin eliminated the cell lines MDA-MB-231 and MDA-MB-436 in a dose-dependent manner. For the cell line MCF7 this tendency was not observed. Furthermore we examined the effects of salinomycin to the CSC-

associated properties of surface marker identity and non-adherent growth of the cell lines MDA-MB-231 and MCF7. The CD24/CD44/CD49f antigenic phenotype was not affected by drug treatment in any of the two cell lines tested. Moreover the spheroid formation in non-adherent environment did not result in treatment-dependent effects on spheroid size or spheroid number. In an additional step, we optimized the soft agar colony formation assay. Finally we successfully tested the methyl cellulose assay, which represents a faster method to produce multicellular aggregates ideal for testing of further downstream spheroid analysis methods.

6.2 Zusammenfassung

Krebsstammzellen (CSCs) stellen eine wichtige Subklasse von neoplastischen Zellen dar und sind von hoher Bedeutung für die Klinik. In dieser Masterarbeit etablierten wir Methoden für die zeitsparende, reproduzierbare Analyse von CSC Eigenschaften, nämlich eine zelloberflächenmarker-basierte, durchflusszytometrische Identifikationsmethode und den Soft-Agar-Koloniebildungs-Test. Es wurden die Oberflächenmarker CD24, CD44 und CD49f ausgewählt und die beiden basalen/mesenchymalen humanen Brustkrebszelllinien MDA-MB-231 und MDA-MB-436 sowie die luminale Brustkrebszelllinie MCF7 verwendet. Mittels der optimierten Bestimmungsmethode wurden die Brustkrebszelllinien bezüglich ihres CD24/CD44/CD49f antigenen Phänotyps charakterisiert. Die Charakterisierung ergab, dass die zwei basal/mesenchymalen Zelllinien MDA-MB-231 und MDA-MB-436 vorwiegend den $CD24^{-}/CD44^{+}/CD49f^{+}$ antigenen Phänotyp aufwiesen. Die luminale Zelllinie MCF7 wies jedoch den $CD24^{+}/CD44^{+}/CD49f^{+}$ antigenen Phänotyp am häufigsten auf. In einem nächsten Schritt wurde der vielversprechende, auf CSC abzielende Wirkstoff Salinomycin verwendet. Die Zytotoxizität von Salinomycin sowie dem Chemotherapeutika Daunorubicin auf die drei Brustkrebszelllinien wurde getestet. Durch eine durchflusszytometrische lebend-tot-Bestimmung wurde gezeigt, dass die Zelllinien MDA-MB-231 und MDA-MB-436 konzentrationsabhängig von Salinomycin getötet wurden. Diese Tendenz konnte aber bei der Zelllinie MCF7 nicht festgestellt werden, wenngleich ein höherer Prozentsatz an toten Zellen als in den anderen Zelllinien nachgewiesen werden konnte. Des Weiteren wurde der Einfluss von Salinomycin auf die mit CSC verbundenen Eigenschaften des Oberflächenmarkerprofils und des nicht-adhärenz

basierten Wachstums der Zelllinien MDA-MB-231 und MCF7 untersucht. Der dominante CD24/CD44/CD49f antigene Phänotyp wurde durch die Behandlung mit Salinomycin in keiner der beiden getesteten Zelllinien beeinflusst. Darüber hinaus konnte kein Zusammenhang zwischen der Fähigkeit der Spheroidbildung (Anzahl, Größe) und den verschiedenen Konditionen festgestellt werden. In einem weiteren Schritt wurde der Soft-Agar-Test optimiert. Als Letztes wurde der alternativ einsetzbare Methylcellulose-Test durchgeführt, welcher eine schnellere Methode zur Generierung von multizellulären Aggregaten darstellt. Dieser Test öffnet die Türen zu Kryoschnitten und Histologie von isolierten multizellulären Aggregaten.

6.3 Curriculum Vitae

Education

Since 10/2013	UNIVERSITY OF VIENNA – MASTER'S PROGRAM BIOLOGICAL CHEMISTRY – FOCUS CHEMICAL BIOLOGY Master's thesis in the MMCT laboratory of Prof. Ogris: "Characterization of potential cancer initiating cells in breast cancer cell lines" Area: Breast Cancer Research
10/2010-09/2013	UNIVERSITY OF INNSBRUCK – BACHELOR'S PROGRAM CHEMISTRY Bachelor thesis with grade 1.0 in the Micura Group: "Synthesis of a preQ1-ligand and the precursor of a phosphoramidite building block" Area: Bioorganic Chemistry Passing Grade: 2.2

09/2004-06/2009	HTL DORNBIRN – CHEMICAL ENGINEERING Graduation with *summa cum laude* Diploma project in cooperation with Getzner Textil AG "Influence of corrosive gases on the yellowing of textile finished, optical brightened and blued cotton fabrics"

Additional Skills

Language Skills:	German – native language English – proficient speaker
Computer Literacy:	Microsoft Office™ (Word™, Excel™ and PowerPoint™), FlowJoe™, ChemBioDraw™, MestReNova™
Assays:	Cancer stem cell marker evaluation using primary antibodies and flow cytometry, non-adherent 3D colony formation assay using soft agar or methyl cellulose, cytotoxicity tests with human breast cancer cells, ELISA
Cell Culture:	Standard bacterial and mammalian cell culture methods S1, knowledge in S2 cell culture work with non-pathogenic lentiviruses

Stipends

10/2014-11/2014	Performance Scholarship University of Vienna

7. References

Abdullah, L.N., Chow, E.K.-H., 2013. Mechanisms of chemoresistance in cancer stem cells. Clin Transl Med 2, 3.

Al-Hajj, M., Wicha, M.S., Benito-Hernandez, A., Morrison, S.J., Clarke, M.F., 2003. Prospective identification of tumorigenic breast cancer cells. Proc. Natl. Acad. Sci. U. S. A. 100, 3983–3988. doi:10.1073/pnas.0530291100

Andersson, B., Janson, V., Behnam-Motlagh, P., Henriksson, R., Grankvist, K., 2006. Induction of apoptosis by intracellular potassium ion depletion: using the fluorescent dye PBFI in a 96-well plate method in cultured lung cancer cells. Toxicol. Vitro Int. J. Publ. Assoc. BIBRA 20, 986–994. doi:10.1016/j.tiv.2005.12.013

Basu, D., Montone, K.T., Wang, L.-P., Gimotty, P.A., Hammond, R., Diehl, J.A., Rustgi, A.K., Lee, J.T., Rasanen, K., Weinstein, G.S., Herlyn, M., 2011. Detecting and targeting mesenchymal-like subpopulations within squamous cell carcinomas. Cell Cycle Georget. Tex 10, 2008–2016.

Benton, G., Kleinman, H.K., George, J., Arnaoutova, I., 2011. Multiple uses of basement membrane-like matrix (BME/Matrigel) in vitro and in vivo with cancer cells. Int. J. Cancer 128, 1751–1757. doi:10.1002/ijc.25781

Bilandzic, M., Stenvers, K.L., 2014. Assessment of Ovarian Cancer Spheroid Attachment and Invasion of Mesothelial Cells in Real Time. J. Vis. Exp. doi:10.3791/51655

Borowicz, S., Van Scoyk, M., Avasarala, S., Karuppusamy Rathinam, M.K., Tauler, J., Bikkavilli, R.K., Winn, R.A., 2014. The Soft Agar Colony Formation Assay. J. Vis. Exp. doi:10.3791/51998

Bortner, C.D., Hughes, F.M., Cidlowski, J.A., 1997. A primary role for K+ and Na+ efflux in the activation of apoptosis. J. Biol. Chem. 272, 32436–32442.

Brenton, J.D., Carey, L.A., Ahmed, A.A., Caldas, C., 2005. Molecular classification and molecular forecasting of breast cancer: ready for clinical application? J. Clin. Oncol. Off. J. Am. Soc. Clin. Oncol. 23, 7350–7360. doi:10.1200/JCO.2005.03.3845

Cariati, M., Naderi, A., Brown, J.P., Smalley, M.J., Pinder, S.E., Caldas, C., Purushotham, A.D., 2008. Alpha-6 integrin is necessary for the tumourigenicity of a stem cell-like subpopulation within the MCF7 breast cancer cell line: Alpha-6 Integrin and Tumourigenicity. Int. J. Cancer 122, 298–304. doi:10.1002/ijc.23103

Chen, K., Huang, Y., Chen, J., 2013. Understanding and targeting cancer stem cells: therapeutic implications and challenges. Acta Pharmacol. Sin. 34, 732–740. doi:10.1038/aps.2013.27

Chow, E.K.-H., Fan, L., Chen, X., Bishop, J.M., 2012. Oncogene-specific formation of chemoresistant murine hepatic cancer stem cells. Hepatology 56, 1331–1341. doi:10.1002/hep.25776

Dong, T.-T., Zhou, H.-M., Wang, L.-L., Feng, B., Lv, B., Zheng, M.-H., 2011. Salinomycin Selectively Targets “CD133+” Cell Subpopulations and Decreases Malignant Traits in Colorectal Cancer Lines. Ann. Surg. Oncol. 18, 1797–1804. doi:10.1245/s10434-011-1561-2

Fillmore, C.M., Kuperwasser, C., 2008. Human breast cancer cell lines contain stem-like cells that self-renew, give rise to phenotypically diverse progeny and survive chemotherapy. Breast Cancer Res. 10, R25. doi:10.1186/bcr1982

Flahaut, M., Meier, R., Coulon, A., Nardou, K.A., Niggli, F.K., Martinet, D., Beckmann, J.S., Joseph, J.-M., Mühlethaler-Mottet, A., Gross, N., 2009. The Wnt receptor FZD1 mediates chemoresistance in neuroblastoma through activation of the Wnt/beta-catenin pathway. Oncogene 28, 2245–2256. doi:10.1038/onc.2009.80

Ghebeh, H., Lehe, C., Barhoush, E., Al-Romaih, K., Tulbah, A., Al-Alwan, M., Hendrayani, S.-F., Manogaran, P., Alaiya, A., Al-Tweigeri, T., others, 2010. Research article Doxorubicin downregulates cell surface B7-H1 expression and upregulates its nuclear expression in breast cancer cells: role of B7-H1 as an anti-apoptotic molecule.

Gilmore, A.P., 2005. Anoikis. Cell Death Differ. 12, 1473–1477. doi:10.1038/sj.cdd.4401723

Gong, C., Yao, H., Liu, Q., Chen, J., Shi, J., Su, F., Song, E., 2010. Markers of Tumor-Initiating Cells Predict Chemoresistance in Breast Cancer. PLoS ONE 5, e15630. doi:10.1371/journal.pone.0015630

Grimshaw, M.J., Cooper, L., Papazisis, K., Coleman, J.A., Bohnenkamp, H.R., Chiapero-Stanke, L., Taylor-Papadimitriou, J., Burchell, J.M., 2008. Mammosphere culture of metastatic breast cancer cells enriches for tumorigenic breast cancer cells. Breast Cancer Res 10, R52.

Gupta, P.B., Onder, T.T., Jiang, G., Tao, K., Kuperwasser, C., Weinberg, R.A., Lander, E.S., 2009. Identification of selective inhibitors of cancer stem cells by high-throughput screening. Cell 138, 645–659. doi:10.1016/j.cell.2009.06.034

Hanahan, D., Weinberg, R.A., 2011. Hallmarks of Cancer: The Next Generation. Cell 144, 646–674. doi:10.1016/j.cell.2011.02.013

Hirsch, H.A., Iliopoulos, D., Tsichlis, P.N., Struhl, K., 2009. Metformin Selectively Targets Cancer Stem Cells, and Acts Together with Chemotherapy to Block Tumor Growth and Prolong Remission. Cancer Res. 69, 7507–7511. doi:10.1158/0008-5472.CAN-09-2994

Keller, P.J., Lin, A., Arendt, L.M., Klebba, I., Jones, A.D., Rudnick, J.A., DiMeo, T.A., Gilmore, H., Jefferson, D.M., Graham, R.A., Naber, S.P., Schnitt, S., Kuperwasser, C., 2010. Mapping the cellular and molecular heterogeneity of normal and malignant breast tissues and cultured cell lines. Breast Cancer Res. 12, R87. doi:10.1186/bcr2755

Kim, W.K., Kim, J.-H., Yoon, K., Kim, S., Ro, J., Kang, H.S., Yoon, S., 2012. Salinomycin, a p-glycoprotein inhibitor, sensitizes radiation-treated cancer cells by increasing DNA damage and inducing G2 arrest. Invest. New Drugs 30, 1311–1318. doi:10.1007/s10637-011-9685-6

Li, H., Liu, L., Guo, L., Zhang, J., Du, W., Li, X., Liu, W., Chen, X., Huang, S., 2008. HERG K+ channel expression in CD34+/CD38-/CD123(high) cells and primary leukemia cells and analysis of its regulation in leukemia cells. Int. J. Hematol. 87, 387–392. doi:10.1007/s12185-008-0056-9

Litman, T., Brangi, M., Hudson, E., Fetsch, P., Abati, A., Ross, D.D., Miyake, K., Resau, J.H., Bates, S.E., 2000. The multidrug-resistant phenotype associated with overexpression of the new ABC half-transporter, MXR (ABCG2). J. Cell Sci. 113 (Pt 11), 2011–2021.

Liu, S., Wicha, M.S., 2010. Targeting breast cancer stem cells. J. Clin. Oncol. Off. J. Am. Soc. Clin. Oncol. 28, 4006–4012. doi:10.1200/JCO.2009.27.5388

Liu, S., Cong, Y., Wang, D., Sun, Y., Deng, L., Liu, Y., Martin-Trevino, R., Shang, L., McDermott, S.P., Landis, M.D., Hong, S., Adams, A., D'Angelo, R., Ginestier, C., Charafe-Jauffret, E., Clouthier, S.G., Birnbaum, D., Wong, S.T., Zhan, M., Chang, J.C., Wicha, M.S., 2014. Breast Cancer Stem Cells Transition between Epithelial and Mesenchymal States Reflective of their Normal Counterparts. Stem Cell Rep. 2, 78–91. doi:10.1016/j.stemcr.2013.11.009

Lu, Y., Ma, W., Mao, J., Yu, X., Hou, Z., Fan, S., Song, B., Wang, H., Li, J., Kang, L., Liu, P., Liu, Q., Li, L., 2015. Salinomycin exerts anticancer effects on human breast carcinoma MCF-7 cancer stem cells via modulation of Hedgehog signaling. Chem. Biol. Interact. 228, 100–107. doi:10.1016/j.cbi.2014.12.002

Manuel Iglesias, J., Beloqui, I., Garcia-Garcia, F., Leis, O., Vazquez-Martin, A., Eguiara, A., Cufi, S., Pavon, A., Menendez, J.A., Dopazo, J., Martin, A.G., 2013. Mammosphere Formation in Breast Carcinoma Cell Lines Depends upon Expression of E-cadherin. PLoS ONE 8. doi:10.1371/journal.pone.0077281

Mitani, M., Yamanishi, T., Miyazaki, Y., 1975. Salinomycin: A new monovalent cation ionophore. Biochem. Biophys. Res. Commun. 66, 1231–1236. doi:10.1016/0006-291X(75)90490-8

Mitani, M., Yamanishi, T., Miyazaki, Y., Otake, N., 1976. Salinomycin effects on mitochondrial ion translocation and respiration. Antimicrob. Agents Chemother. 9, 655–660.

Mueller, M.-T., Hermann, P.C., Witthauer, J., Rubio-Viqueira, B., Leicht, S.F., Huber, S., Ellwart, J.W., Mustafa, M., Bartenstein, P., D'Haese, J.G., Schoenberg, M.H., Berger, F., Jauch, K.-W., Hidalgo, M., Heeschen, C., 2009. Combined targeted treatment to eliminate tumorigenic cancer stem cells in human pancreatic cancer. Gastroenterology 137, 1102–1113. doi:10.1053/j.gastro.2009.05.053

Naujokat, C., Steinhart, R., 2012. Salinomycin as a Drug for Targeting Human Cancer Stem Cells. J. Biomed. Biotechnol. 2012, 1–17. doi:10.1155/2012/950658

Noda, T., Nagano, H., Takemasa, I., Yoshioka, S., Murakami, M., Wada, H., Kobayashi, S., Marubashi, S., Takeda, Y., Dono, K., Umeshita, K., Matsuura, N., Matsubara, K., Doki, Y., Mori, M., Monden, M., 2009. Activation of Wnt/beta-catenin signalling pathway induces chemoresistance to interferon-alpha/5-fluorouracil combination therapy for hepatocellular carcinoma. Br. J. Cancer 100, 1647–1658. doi:10.1038/sj.bjc.6605064

O'Shaughnessy, J., 2005. Extending survival with chemotherapy in metastatic breast cancer. The oncologist 10, 20–29.

Pang, B., Qiao, X., Janssen, L., Velds, A., Groothuis, T., Kerkhoven, R., Nieuwland, M., Ovaa, H., Rottenberg, S., van Tellingen, O., Janssen, J., Huijgens, P., Zwart, W., Neefjes, J., 2013. Drug-induced histone eviction from open chromatin contributes to the chemotherapeutic effects of doxorubicin. Nat. Commun. 4, 1908. doi:10.1038/ncomms2921

Park, C.Y., Tseng, D., Weissman, I.L., 2009. Cancer Stem Cell–Directed Therapies: Recent Data From the Laboratory and Clinic. Mol. Ther. 17, 219–230. doi:10.1038/mt.2008.254

Park, J.H., Park, S.J., Chung, M.K., Jung, K.H., Choi, M.R., Kim, Y., Chai, Y.G., Kim, S.J., Park, K.S., 2010. High expression of large-conductance Ca2+-activated K+ channel in the CD133+ subpopulation of SH-SY5Y neuroblastoma cells. Biochem. Biophys. Res. Commun. 396, 637–642. doi:10.1016/j.bbrc.2010.04.142

Pressman, B.C., Lattanzio, F.A., 1978. Cardiovascular effects of ionophores, in: Frontiers of Biological Energetics. Academic Press, New York, pp. 1245–1252.

Reya, T., Morrison, S.J., Clarke, M.F., Weissman, I.L., 2001. Stem cells, cancer, and cancer stem cells. Nature 414, 105–111. doi:10.1038/35102167

Riaz, M., Elstrodt, F., Hollestelle, A., Dehghan, A., Klijn, J.G., Schutte, M., 2009. Low-risk susceptibility alleles in 40 human breast cancer cell lines. BMC Cancer 9, 236. doi:10.1186/1471-2407-9-236

Riccioni, R., Dupuis, M.L., Bernabei, M., Petrucci, E., Pasquini, L., Mariani, G., Cianfriglia, M., Testa, U., 2010. The cancer stem cell selective inhibitor salinomycin is a p-glycoprotein inhibitor. Blood Cells. Mol. Dis. 45, 86–92. doi:10.1016/j.bcmd.2010.03.008

Ruddon, R.W., 2003. What Makes a Cancer Cell a Cancer Cell?

Sakakibara, M., Fujimori, T., Miyoshi, T., Nagashima, T., Fujimoto, H., Suzuki, H.T., Ohki, Y., Fushimi, K., Yokomizo, J., Nakatani, Y., Miyazaki, M., 2012. Aldehyde dehydrogenase 1-positive cells in axillary lymph node metastases after chemotherapy as a prognostic factor in patients with lymph node-positive breast cancer. Cancer 118, 3899–3910. doi:10.1002/cncr.26725

Scharenberg, C.W., Harkey, M.A., Torok-Storb, B., 2002. The ABCG2 transporter is an efficient Hoechst 33342 efflux pump and is preferentially expressed by immature human hematopoietic progenitors. Blood 99, 507–512.

Shapiro, A.B., Corder, A.B., Ling, V., 1997. P-glycoprotein-mediated Hoechst 33342 transport out of the lipid bilayer. Eur. J. Biochem. FEBS 250, 115–121.

Sreerama, L., Sladek, N.E., 1997. Cellular levels of class 1 and class 3 aldehyde dehydrogenases and certain other drug-metabolizing enzymes in human breast malignancies. Clin. Cancer Res. Off. J. Am. Assoc. Cancer Res. 3, 1901–1914.

Steinhart, R., Berghauser, K.H., Steinhart, B., Martschoke, C., Hojer, L., Naujokat, C., 2012. Breast cancer metastasis regression by salinomycin. Case Reports in Oncology.

Zhang, G.-N., Liang, Y., Zhou, L.-J., Chen, S.-P., Chen, G., Zhang, T.-P., Kang, T., Zhao, Y.-P., 2011. Combination of salinomycin and gemcitabine eliminates pancreatic cancer cells. Cancer Lett. 313, 137–144. doi:10.1016/j.canlet.2011.05.030

Zhang, Y., Zhang, H., Wang, X., Wang, J., Zhang, X., Zhang, Q., 2012. The eradication of breast cancer and cancer stem cells using octreotide modified paclitaxel active targeting micelles and salinomycin passive targeting micelles. Biomaterials 33, 679–691. doi:10.1016/j.biomaterials.2011.09.072

Zhou, B.-B.S., Zhang, H., Damelin, M., Geles, K.G., Grindley, J.C., Dirks, P.B., 2009. Tumour-initiating cells: challenges and opportunities for anticancer drug discovery. Nat. Rev. Drug Discov. 8, 806–823. doi:10.1038/nrd2137